Targeting CSF-1 ameliorates experimental autoimmune encephalomyelitis by depleting inflammatory monocytes and microglia in the central nervous system without affecting quiescent microglia.

Daniel Hwang[1], Larissa Lumi Watanabe Ishikawa[1], Alexandra Boehm[1], Ziver Sahin[1], Giacomo Casella[1], Soohwa Jang[1], Maryamsadat Seyedsadr[1], Michael V. Gonzalez[2], James P. Garifallou[2], Hakon Hakonarson[2,3], Guang-Xian Zhang[1], Abdolmohamad Rostami[1], and Bogoljub Ciric[1,*]

[1]Department of Neurology, Jefferson Hospital for Neuroscience, Thomas Jefferson University, Philadelphia, PA.
[2]Center for Applied Genomics, The Children's Hospital of Philadelphia, Abramson Research Center, Philadelphia, PA, 19104.
[3]Department of Pediatrics, Perelman School of Medicine, University of Pennsylvania, Philadelphia PA, 19104

*Corresponding author: Bogoljub Ciric, Ph.D., Associate Professor, Department of Neurology, Jefferson Hospital for Neuroscience, Thomas Jefferson University, 900 Walnut Street, Suite 300, Philadelphia, PA, 19107. bogoljub.ciric@jefferson.edu

Short title: Blocking CSF-1 ameliorates EAE.

ABSTRACT

Multiple sclerosis (MS) and its model, experimental autoimmune encephalomyelitis (EAE), are autoimmune diseases characterized by extensive infiltration of myeloid cells into the central nervous system (CNS). Although myeloid cells are essential to MS/EAE pathology, none of the current MS therapies specifically target them. A promising strategy for bridging this gap may be targeting the biological activity of CSF-1R, a receptor tyrosine kinase important for survival and functioning of certain myeloid cells, such as monocytes and macrophages. It has been shown that CSF-1R inhibitors suppress EAE, but it is not known whether targeting CSF-1R ligands, CSF-1 and IL-34, could be a viable therapeutic strategy. We found that neutralization of CSF-1 with Ab attenuates ongoing EAE, similar to CSF-1R inhibitor BLZ945, whereas neutralization of IL-34 had no effect. Both anti-CSF-1- and BLZ945-treated mice with EAE had greatly diminished numbers of monocyte-derived dendritic cells and microglia in the CNS. However, anti-CSF-1 antibody selectively depleted inflammatory microglia, whereas BLZ945 depleted virtually all microglia, including quiescent microglia. We also found depletion of myeloid cells in the spleen and lymph nodes of anti-CSF-1- and BLZ945-treated mice, but only a modest decrease in encephalitogenic T cell responses, suggesting that the depletion of CNS myeloid cells is more relevant to EAE suppression. Decreased myeloid cell populations in treated mice resulted in reduced production of IL-1β, a key inflammatory mediator in EAE. The treatments also reduced the frequencies of CCL2- and CCR2-expressing cells in the CNS, suggesting that CSF-1/CSF-1R inhibition may hinder recruitment of immune cells to the CNS. Our findings suggest that targeting CSF-1 may be effective in ameliorating myeloid cell-mediated MS pathology, while preserving homeostatic functions of microglia and decreasing risks that might arise from their ablation with small molecule inhibitors of CSF-1R.

INTRODUCTION

Multiple sclerosis (MS) is an autoimmune disease characterized by accumulation of immune cells in inflamed areas of the central nervous system (CNS), which form demyelinated regions called MS lesions [2]. Myeloid cells account for up to 85% of immune cells in active MS lesions [3-5], suggesting that they are the major mediators of pathology in MS. In support of this notion, studies in an animal model of MS, experimental autoimmune encephalomyelitis (EAE), have demonstrated the essential role of myeloid cells in EAE pathology, as interventions that affect them, in particular monocytes and conventional dendritic cells (cDCs), ameliorate or abrogate EAE [6-8]. However, despite the evidence on the importance of myeloid cells in CNS autoimmunity, myeloid cells have not thus far been specifically targeted for MS therapy. This provides an opportunity for devising therapeutic approaches that target myeloid cells relevant to MS pathology.

Receptor for colony stimulating factor 1 (CSF-1R) is a cell-surface receptor tyrosine kinase that binds two ligands, CSF-1 and IL-34 [9]. CSF-1R signaling facilitates survival and proliferation of myeloid cells, with either CSF-1 or IL-34 predominantly controlling the population size of various myeloid cells in different organs and tissues [9-11]. CSF-1R is expressed on microglia, monocytes and monocyte-derived cells, which comprise the bulk of myeloid cells in the CNS during MS and EAE [10]. It has been shown that inhibition of CSF-1R signaling with small molecule inhibitors suppresses EAE pathology [12, 13], but the effects of CSF-1R inhibition on particular myeloid cell subsets relevant in EAE remain poorly understood. Further, different methods for blocking CSF-1R signaling in EAE, such as by antibodies (Ab) against the receptor and its individual ligands have not been compared with small molecule inhibitors. The principal difference between these blocking methods is that small molecule inhibitors readily penetrate the CNS [1], whereas Abs do not [10, 14], a difference that can lead to distinct therapeutic outcomes, given that the types and numbers of myeloid cells affected by the inhibition can vary substantially. In addition, any indirect effects of CSF-1R inhibition on cells that do not express CSF-1R also remain largely uncharacterized.

Our data and other studies show that small molecule inhibitors of CSF-1R cause a profound depletion of microglia [1, 10], which may be an important drawback in their use for therapy, as microglia play important roles in CNS homeostasis [15]. It has been shown that neurons can express CSF-1R during excitotoxic injury,

contributing to the survival of injured neurons [15]. Notably, it remains unknown whether neurons express CSF-1R in EAE and MS. Thus, the ideal MS therapy targeting CSF-1R would preferentially affect inflammatory myeloid cells, while sparing cells with homeostatic functions, such as quiescent microglia. This may be accomplished by targeting CSF-1R ligands, CSF-1 and IL-34, which show spatial and context- dependent differences in expression [16]. CSF-1 is systemically the dominant CSF-1R ligand, with its concentrations in the serum being approximately ten times greater than that of IL-34 [17-23]. Importantly, CSF-1 is not highly expressed in the CNS, but its expression can be upregulated by inflammation or injury [24], facilitating expansion of myeloid cells at the site of inflammation. In contrast to more widespread CSF-1 expression, IL-34 is primarily and constitutively expressed in the CNS and skin [25, 26]. In steady state, IL-34 maintains survival of tissue-resident myeloid cells in the skin and CNS, as the primary deficiency of IL-34 knockout mice is lack of Langerhan's cells and microglia, respectively [16]. IL-34 is the predominant CSF-1R ligand in the CNS, accounting for 70% of total CSF-1R signaling in healthy brain [15].

In the present study, we sought to understand how CSF-1R inhibition affects immune cells in the CNS of mice with EAE, and to determine how the effects of blocking CSF-1 and IL-34 may differ from blockade of CSF-1R. We found that treatment with CSF-1R inhibitor BLZ945 suppresses EAE when given both prophylactically and therapeutically. Treatment efficacy correlated with a dramatic reduction in the numbers of monocytes, monocyte-derived dendritic cells (moDCs), and microglia, suggesting that loss of one or more of these cell types is responsible for EAE suppression. We also found that Ab-mediated blockade of CSF-1, but not of IL-34, suppressed EAE. Notably, anti-CSF-1 treatments preferentially depleted inflammatory myeloid cells, whereas quiescent microglia were preserved. These findings suggest that blockade of CSF-1, rather than of CSF-1R, may be a preferable therapeutic strategy for alleviating myeloid cell-mediated pathology in MS.

RESULTS

Blocking CSF-1R or CSF-1, but not IL-34, suppresses EAE development.

To determine the role of CSF-1R, CSF-1, and IL-34 in EAE development, we blocked them with either a small-molecule inhibitor, or neutralizing MAbs. We blocked CSF-1R function with BLZ945, a brain-penetrant small-molecule inhibitor of CSF-1R kinase activity that, among other effects, potently depletes microglia within 5-7 days of treatment [1]. Oral treatment with BLZ945 delayed the onset of EAE for 6-15 days when given prophylactically (Fig. 1A). BLZ945 initially suppressed disease severity (Fig. 1A), but animals eventually developed progressively severe disease despite continuous treatment with BLZ945. We also blocked CSF-1R activity with neutralizing MAb, which was less efficacious than BLZ945 in delaying EAE onset, and only modestly reduced disease severity (Fig. 1B). Surprisingly, anti-CSF-1R MAb failed to bind to microglia, as determined by flow cytometry, whereas it bound to monocytes (Supplemental Fig. 1C). Given that microglia express CSF-1R [27, 28] and are dependent on it for survival [29], it is unclear why AFS98 MAb does not bind to microglia, and how that may have impacted its effect in EAE.

We then tested how blocking either CSF-1 or IL-34 with MAbs would affect EAE. In contrast to blocking CSF-1R, blocking of CSF-1 did not delay onset of disease (Fig. 1C) but did persistently suppress disease severity over the course of treatment, including for over 40 days (Fig. 4B). Unlike anti-CSF-1 treatment, anti-IL-34 treatments did not influence either EAE onset or severity (Fig. 1D). We tested whether our treatments with the MAbs, which were rat IgGs, induced an anti-rat IgG response in treated mice. Anti-CSF1, and control rat IgG2a isotype MAb induced similar low titers of anti-rat IgG in treated mice, whereas anti-CSF-1R and anti-IL-34 MAbs induced a notably higher anti-rat IgG response (Supplementary Fig. 1B). This indicates that anti-rat IgG responses in treated mice could have reduced neutralizing effects of injected MAbs, especially in the case of anti-CSF-1R and anti-IL-34 MAbs. Even so, this would occur with a delay, as anti-rat IgG Ab titers would build up gradually.

To minimize the development of anti-rat IgG responses against the anti-IL-34 MAb, we treated mice with anti-IL-34 MAb immediately after the onset of clinical disease; however, this treatment had no impact on disease as well (Supplemental Fig. 1D). We also tested whether administration of recombinant CSF-1 could exacerbate EAE pathology, but i.p. injections of CSF-1 did not worsen EAE (Supplementary Fig. 1A). Overall, these data

show that blocking CSF-1R signaling attenuates the severity of EAE, and that CSF-1, but not IL-34, is the relevant CSF-1R ligand in EAE.

Prophylactic BLZ945 treatment depletes myeloid antigen-presenting cells in the CNS of mice with EAE. We characterized how CSF-1R inhibition with BLZ945 influenced CNS inflammation at the peak of EAE. BLZ945-treated animals had ~90% reduced numbers of $CD45^+$ cells in the CNS compared to vehicle-treated animals (Fig. 2A). All major lineages of immune cells were reduced in number, including $CD11b^+$, $CD11c^+$ and $CD4^+$ cells (Supplementary Fig. 2A). $CD11b^+$ cells were most dramatically impacted, including profound depletion of $CD45^{Low}CD11b^+Tmem119^+CX3CR1^{Hi}$ microglia (Supplementary Fig. 2E, F), as reported for BLZ945 treatment [1]. Amongst $CD45^{Hi}$ cells, there was significant reduction in the frequency of $CD11b^+CD11c^+$ myeloid DCs (Supplementary Fig. 2B). Myeloid DCs in the CNS of mice with EAE primarily comprise moDCs, and indeed $CD45^{Hi}$ $CD11b^+$ $CD11c^+$ $Ly6G^{Low/-}Ly6C^{Hi}$ MHC II^{Hi} moDCs were nearly absent from the CNS of BLZ945-treated mice (Supplementary Fig. C,D). We also found several differences in cytokine production by $CD4^+$ T cells from BLZ945-treated mice, including higher frequencies of IL-10^+ and TNF^+ cells, and lower frequency of GM-CSF^+ cells (Supplementary Fig. 2G).

To comprehensively define how CSF-1R inhibition influences the overall composition of immune cells in the CNS during EAE, we analyzed flow cytometry data by *t*-stochastic neighbor embedding (*t*-SNE). Consistent with manual gating, the frequency of microglia and moDCs/macrophages was dramatically reduced (Fig. 2B-F). In contrast, the frequency of neutrophils was increased; likely reflecting that they do not express CSF-1R [30], and are therefore not impacted by CSF-1R inhibition. Interestingly, the frequency of undifferentiated monocytes ($CD45^{Hi}CD11b^+Ly6C^{Hi}CD11c^-MHCII^-$) increased, suggesting that CSF-1R may impact monocyte differentiation. Overall, BLZ945 treatment markedly reduced the frequency of $CD11c^+$ myeloid antigen-presenting cells (APCs) expressing MHC class II, CD80 and CD86 (Fig. 2E,F), suggesting that CSF-1R signaling maintains sufficient numbers of APCs in the CNS to drive inflammation during EAE.

BLZ945 suppresses EAE when given therapeutically, reducing the number of myeloid APCs in the CNS.

We next tested whether BLZ945 could suppress EAE after clinical disease has developed, as that scenario is the most relevant to MS therapies. Therapeutic treatments with BLZ945 rapidly suppressed clinical EAE in a dose-dependent manner, with 300 mg/kg/day dose being the most efficacious (Fig 3A-B). To determine the acute effects of CSF-1R inhibition on immune cells in the CNS, we focused our analysis on mice treated with BLZ945 for 6 days, starting at a clinical score of 2.0. Compared to control mice, BLZ945-treated mice had reduced numbers of $CD45^+$ cells in the CNS (Fig. 3C), primarily due to fewer $CD11b^+$ and $CD11c^+$ cells, whereas the numbers of $CD4^+$ cells were mostly unaffected (Fig. 3D). Fewer numbers of $CD11b^+$ cells reflect depletion of microglia and reduction in numbers of $CD11b^+CD11c^+$ cells among infiltrating $CD45^{Hi}$ cells (Fig. 3E). In contrast, $CD11b^+CD11c^-$ cells were not affected by BLZ945 treatment (Fig. 3F). Most immune cells depleted by BLZ945 treatment co-expressed CD11c, TNF, MHC II, CD80, and CD86, suggesting that inflammatory APCs are preferentially affected by CSF-1R inhibition (Fig. 3G-I). Taken together, these data further indicate that inhibition of CSF-1R signaling reduces the pool of APCs in the CNS during EAE. Moreover, this bolster the notion that targeting CSF-1R signaling is therapeutically efficacious in EAE, by reducing myeloid cell-dependent inflammation.

Blockade of CSF-1 with MAb depletes inflammatory myeloid APCs in the CNS during EAE, but does not affect quiescent microglia.

We next tested the therapeutic efficacy of anti-CSF-1 MAb treatment. The treatment initiated after onset of disease suppressed clinical EAE (Fig. 4A) and the suppression was maintained up to 45 days after EAE induction, which was the longest period tested (Fig. 4B). Similar to BLZ945, anti-CSF-1 MAb suppressed disease even when treatments were initiated during its more advanced stage (Fig. 4C, D). Mice treated with anti-CSF-1 MAb had fewer immune cells in the CNS, including $CD11b^+$, $CD11c^+$, and $CD4^+$ cells (Fig. 4E, F). The treatments significantly decreased frequency of $CD11b^+CD11c^+$ myeloid DCs in the CNS (Supplementary Fig. 3A) and among $CD11b^+$ myeloid cells, we observed reduced frequencies of $CD11c^+$ microglia, moDCs, cDCs and other $CD11c^+$ cells, indicating that DC populations were preferentially affected (Supplementary Fig. 3B). Of relevance to therapy, anti-CSF-1 MAb treatments reduced the numbers of microglia to those in naïve mice (Fig. 4G), without depleting almost entire microglia, as BLZ945 does. This suggests that CSF-1 promotes the expansion of

activated microglia in response to inflammation. Consistent with this hypothesis, the reductions in microglia numbers in anti-CSF-1-treated mice were primarily due to loss of activated microglia, which expressed MHC II and/or CD68 (Fig. 4H).

We then quantified how anti-CSF-1 MAb treatments affected the composition of myeloid cells in the inflamed CNS by analyzing $CD45^+CD11b^+$ cells from isotype- and anti-CSF-1-treated animals by *t*-SNE (Fig. 4I,J). Anti-CSF-1 treatments reduced the frequencies of moDCs, macrophages, activated microglia and undifferentiated monocytes, but did not affect the frequency of neutrophils. This resulted in a large increase in the frequency of quiescent microglia among $CD11b^+$ cells. Similar to BLZ945-treated mice, anti-CSF-1 MAb treatment resulted in MFI decrease for MHC II and CD80, but not CD86 (Fig. 4K), suggesting that inflammatory APCs were impacted by anti-CSF-1 MAb treatments. Consistent with this, anti-CSF-1-treated mice had a lower frequency of $TNF^+MHC\ II^+$ cells in their CNS (Supplementary Fig. 3C). As in BLZ945-treated animals, numbers of moDCs were dramatically reduced by anti-CSF-1 treatment (Supplementary Fig. 3D). An important pathogenic function of moDCs in EAE is production of IL-1β [31]. As expected, a reduced frequency of IL-1β-producing cells was also observed in the CNS of anti-CSF-1 treated EAE mice (Fig. 4L). Together, these data suggest that blockade of CSF-1 preferentially depletes infiltrating and resident inflammatory myeloid cells, without affecting the homeostatic pool of microglia.

CSF-1R inhibition depletes myeloid DCs and monocytes in peripheral lymphoid compartments.

Treatment with BLZ945 delayed onset of disease, while anti-CSF-1 treatment did not. This difference could be due to diminished priming of encephalitogenic T cell responses in peripheral lymphoid organs of BLZ945-treated mice, resulting in failure to initiate disease in the CNS. To test this possibility, we treated immunized mice with either BLZ945 or anti-CSF-1 MAb and sacrificed them during the priming phase of EAE on day 8 p.i. We quantified the immune cells in blood, draining lymph nodes (dLN) and spleen, and found no difference in overall numbers of $CD45^+$ cells in any tissues examined from BLZ945- or anti-CSF-1-treated mice compared to control animals (Supplementary Fig. 4). We did, however, observe a decrease in the numbers of $CD11b^+$ cells in all tissues examined from BLZ945-treated mice, but not from anti-CSF-1-treated mice (Supplementary Fig. 4A-C). Further examination of $CD11b^+$ cells revealed fewer $CD11b^+CD11c^+$ cells in the spleen, blood and dLN from

BLZ945-treated mice (Fig. 5A-C), and in the spleen and blood of anti-CSF-1-treated mice (Fig. 5D-F). Similarly, there was a decrease in moDCs in most secondary lymphoid organs from both BLZ945- and anti-CSF-1-treated mice (Fig. 5A-F). Notably, numbers of monocytes were reduced in all examined tissues from BLZ945-treated mice, but not from anti-CSF-1-treated mice (Fig. 5). We tested whether reductions in myeloid DCs in the spleen and dLNs would diminish MOG_{35-55}-specific T cells responses, but did not find reduced proliferation of cells from either BLZ945- or anti-CSF-1-treated animals when compared to control animals (Fig. 5G,H). We also measured antigen-specific proliferation at day 16 p.i. and found a reduction in proliferation of splenocytes from BLZ945-treated mice, but not of cells from dLNs (Fig. 5I,J). The reduction was likely due to fewer APCs, rather than intrinsic differences in APC function, as co-culture of equal numbers of $CD11c^+$ cells purified from spleens of vehicle- or BLZ945-treated mice with $CD4^+$ T cells from 2D2 mice elicited similar levels of proliferation. These data show that myeloid DCs are impacted by CSF-1R inhibition, but this only modestly affected the development of myelin antigen-specific responses. Thus, delayed onset of disease in BLZ945-treated animals is likely due to factors other than impaired development of MOG_{35-55}-specific T cells responses.

CSF-1R signaling promotes survival/proliferation of BM-derived moDCs but not their APC function.

We sought to understand how CSF-1R signaling influences the numbers of DCs using BMDC cultures, generated in the presence of GM-CSF and neutralizing anti-CSF-1 and anti-CSF-1R MAbs. It has been shown that there is a large expansion of monocyte precursors in these cultures and that resulting DCs are predominantly monocyte-derived [32]. We found that cultures with either anti-CSF-1 or anti-CSF-1R MAbs contained fewer $CD11c^+MHCII^{Hi}$ DCs (Fig. 6A). This was coincidental with a decreased ratio of live/dead cells after LPS treatment (Fig. 6B), suggesting that survival of BMDCs was negatively impacted by the absence of CSF-1R signaling. We also tested whether CSF-1R signaling was important for development of APC function in BMDCs. We observed only a small reduction in the frequency of $CD11c^+MHCII^+$ among live $CD11b^+$ cells (Fig. 6C,D), suggesting that CSF-1R inhibition affects numbers of BMDCs, rather than their ability to differentiate in the presence of GM-CSF and IL-4. To test this hypothesis, we then determined whether CSF-1R inhibition influences APC function of BMDCs by co-culturing them with 2D2 $CD4^+$ T cells. Blocking CSF-1R signaling, either during differentiation/maturation of BMDCs, or during the co-culturing, did not affect the proliferation of 2D2 T cells (Fig. 6E). To confirm that these findings are applicable to monocyte-derived BMDCs, we purified $CD11b^+Ly6G^-Ly6C^{Hi}$ monocytes from the BM

of CD45.1^{+} mice, mixed them with total BM cells from CD45.2^{+} mice and then blocked CSF-1R signaling during their development into BMDCs. Consistent with total BM cultures, blockade of CSF-1R signaling did not affect the frequency of CD11c^{+}MHCII^{Hi}CD45.1^{+} monocyte-derived cells (Fig. 6F,G), but it caused a ~75% reduction in their numbers when compared to control IgG-treated cultures (Fig. 6H). Together, these data indicate that CSF-1R signaling promotes the survival of moDCs, rather than promoting their differentiation and APC function, which is consistent with the role of CSF-1R signaling in maintaining myeloid cell populations [9-11].

Blocking CSF-1R signaling or CSF-1 reduces numbers of CCL2-producing and CCR2-expressing myeloid cells in the CNS during EAE.

We observed that numbers of monocytes/moDCs were greatly reduced in the CNS of mice with EAE during CSF-1R inhibition. Given that monocyte recruitment into the CNS via CCL2/CCR2 signaling is essential to EAE pathology [33, 34], and that several reports have shown that CSF-1 induces CCL2 production by monocytes [35-37], we examined CCL2 production in the CNS of BLZ945- and anti-CSF-1-treated mice with EAE. The vast majority of CCL2^{+} cells were CD45^{+} (Supplementary Fig. 5A). Among CD45^{+} cells, there was a reduction in numbers of CCL2^{+} cells in both BLZ945- and anti-CSF-1-treated animals (Fig. 7A, D). The majority of CCL2^{+} cells was CD11b^{+}Ly6C^{+} (Fig 7B,C,E,F), indicating that monocyte-derived cells are a relevant source of CCL2 in the CNS during EAE. Most CCL2^{+} cells were TNF^{+}MHC II^{+} inflammatory myeloid cells (Supplementary Fig. 5B,C,F,G). Notably, MFI for CCL2 among CCL2^{+} cells from anti-CSF-1-treated mice but not from BLZ945-treated mice was also reduced (Supplementary Fig. 5E).

We also examined CCR2^{+} cells from the CNS of BLZ945- and anti-CSF-1-treated mice. As with CCL2-producing cells, there was a reduction in numbers of CCR2^{+} cells (Fig. 7G,J). Most CCR2^{+} cells were CD45^{Hi}CD11b^{+}Ly6C^{+} cells (Fig. 7H,I,K,L), indicating that these were the same cells that produce CCL2. Indeed, nearly all CCL2^{+} cells were CCR2^{+}CD11b^{+} cells in anti-CSF-1-treated mice (Supplementary Fig. 5K). Combined with our *in vitro* findings, these data suggest that antagonism of CSF-1R signaling inhibits the survival and proliferation of monocytes/moDCs, resulting in fewer CCL2-producing cells, which then reduces the recruitment of CCR2^{+} cells in the CNS during EAE.

Monocytes remaining in the CNS of anti-CSF-1-treated mice have a transcriptional profile consistent with a pro-survival phenotype.

Anti-CSF-1 MAb treatments depleted most (>80% depletion) but not all monocytes and monocyte-derived cells in the CNS of mice with EAE (Fig. 8A,B). To identify transcriptional changes that could have enabled some monocytes to persist despite diminished CSF-1 signaling, we sequenced their transcriptome after 6 days of treatment, a timepoint that correlated well with maximal disease suppression (gating strategy shown in Supplementary Fig. 6A). There were 412 genes differentially expressed between monocytes from anti-CSF-1- and control MAb-treated mice (Fig. 8C,D). We utilized the DAVID bioinformatics database [38, 39] to identify gene ontology, and KEGG pathway terms that were significantly enriched among the differentially expressed genes. Among GO terms identified as significantly enriched, the largest percentage of genes were involved in cell division (Fig. 8E and Supplementary Fig. 6B). Among enriched KEGG pathways in these monocytes, the module with the greatest number of genes was the PI3K-Akt signaling pathway (Fig. 8F and Supplementary Fig. 6C), which controls proliferation [40]. Among genes in this pathway, a number of growth factor receptors and transcription factors were upregulated, including VEGFR, myb, Kit, Pdgfrb, and Fgfr1 (Fig. 8G). These data suggest that monocytes in the CNS of anti-CSF-1-treated mice survive by upregulation of alternative growth factor receptors, which compensate for diminished CSF-1R signaling.

DISCUSSION

We show that blocking CSF-1R, CSF-1 and IL-34 has differential effects on EAE. Overall, inhibition of CSF-1R signaling by blocking either CSF-1R or CSF-1 resulted in suppression of clinical disease and diminished numbers of inflammatory myeloid cells in the CNS. Numbers of microglia and monocyte-derived cells were reduced by CSF-1R inhibition. Notably, blocking CSF-1R or CSF-1 produced distinct effects on the composition of immune cells in the CNS during EAE. Treatment with BLZ945 depleted almost all microglia, whereas anti-CSF-1 MAb treatment preferentially depleted inflammatory microglia, reducing their number to similar levels as in naïve mice. This limited depletion of microglia by anti-CSF-1 MAb could be advantageous in MS therapy, as it carries fewer potential risks than widespread microglia depletion likely would. Of importance for MS therapy, notably lower microglia depletion by anti-CSF-1 MAb than with BLZ945 did not result in an inferior disease suppression, but rather improved long-term therapeutic efficacy when compared to BLZ945 treatments, suggesting that full therapeutic benefit can be achieved without applying a maximally ablative approach.

The limited microglia depletion by anti-CSF-1 MAb is likely due to the presence of IL-34 in non-inflamed CNS areas, where it maintains homeostatic microglia survival. Indeed, it has been shown that systemic anti-CSF-1 MAb injections do not deplete microglia [41], which is consistent with studies showing that IL-34 accounts for approximately 70% of CSF-1R signaling in healthy brain [15]. Moreover, anti-CSF-1 MAb are unlikely to penetrate extensively into the CNS parenchyma, as only a miniscule fraction of Abs cross the intact blood-brain-barrier [10, 14]. Thus, it is expected that neutralization of CSF-1 in the CNS occurs primarily in active lesions, resulting in localized depletion of inflammatory myeloid cells. This model is analogous to the role of CSF-1R ligands in the skin, where IL-34 maintains Langerhans cells in steady state. However, during skin inflammation IL-34 becomes dispensable, as infiltrated immune cells produce CSF-1 and maintain/expand numbers of Langerhans cells [25]. It should be noted, however, that CSF-1R signaling is not in itself inherently pro-inflammatory by eliciting inflammatory phenotype of myeloid cells, but can have such a net effect by simply maintaining their survival during inflammation. In fact, in the absence of inflammation, CSF-1R signaling induces a suppressive M2 phenotype in macrophages and a resting/quiescent phenotype in microglia [1, 15, 19, 42-54]. Hence, our observations on blockade of CSF-1R signaling in EAE are the net effect of abrogating both pro- and anti-inflammatory functions of CSF-1R signaling, with the pro-inflammatory ones predominating. Together, our

findings suggest that CSF-1 promotes inflammation in EAE by expansion of microglia and monocyte-derived myeloid cells, whereas IL-34 maintains microglia in non-inflamed CNS areas, similar to the healthy CNS.

Our data suggest that IL-34 does not play a significant role in EAE. This can be explained by notably more widespread and abundant expression of CSF-1 compared with IL-34 [55]. In most cases CSF-1 can therefore compensate for lack of IL-34. This interpretation is supported by the striking differences in phenotypes of CSF-1 and IL-34 knockout mice, with CSF-1 knockout mice having numerous severe defects, whereas IL-34 knockout mice have mild phenotype [16]. Observations that CSF-1 is present in serum in surprisingly high concentrations (~500-1000 pg/ml) [17-20], which is approximately 10 times higher than IL-34 (~50-100 pg/ml) [21-23], further support the view that CSF-1 is more plentiful than IL-34 and is therefore more impactful. Moreover, a study has demonstrated that CSF-1 in inflamed sites becomes the dominant CSF-1R ligand, even in tissue (skin) where IL-34, but not CSF-1, is expressed in steady state [25]. Thus, although our data suggest that blockade of IL-34 with rat MAb may have been incomplete due to the development of anti-rat IgG responses, it is probable that abundantly produced CSF-1 in CNS lesions mediates most CSF-1R signaling, and that blockade of IL-34 therefore does not have any effect on EAE.

Our in vitro studies with BMDCs and moDCs show that the primary effect of CSF-1R inhibition is limiting the number of myeloid DCs in these cultures rather than affecting their APC functions. These data are consistent with a body of literature showing that CSF-1R signaling in myeloid cells chiefly provides proliferative and anti-apoptotic signals for maintenance of the population size as regulated by ligand availability [56]. This concept is exemplified by differences between animals lacking CSF-1 and IL-34, in which CSF-1 knockout mice have reduced numbers of osteoclasts and monocytes but only a modest reduction in microglia [16]. In contrast, IL-34 knockout mice have greatly reduced numbers of microglia and Langerhans cells, but largely normal numbers of other tissue resident macrophages [16]. Thus, CSF-1R inhibition is likely to suppress inflammation in EAE by reducing the population size of inflammatory myeloid cells in the CNS.

Transcriptional profiling of the remaining monocytes from the CNS of mice treated with anti-CSF-1 MAb suggests that they avoid death from lack of CSF-1R signaling via upregulation of other growth factor receptors known to

promote myeloid cell survival, including Kit [57-59]. Notably, upregulation of these genes has been reported in myeloid cell cancers [60-64]. However, a number of questions regarding these surviving monocytes remain, such as: are they a normally present subpopulation among CNS monocytes, or they are induced by blockade of CSF-1; do they eventually succumb to early death compared to those monocytes that have been receiving CSF-1R signaling; do all monocytes lacking CSF-1R signaling temporarily acquire this phenotype before death; and, what is the capacity of the surviving monocytes to perpetuate inflammation? It is possible that altered phenotype of surviving monocytes is less pro-inflammatory because of diminished effector functions, such as cytokine and chemokine production.

Our in vivo studies indicate an additional mechanism of EAE suppression by inhibition of CSF-1R signaling, namely reduced recruitment of cells to the CNS. We found reduction in numbers of both CCL2- and CCR2-expressing cells when mice with EAE were treated with BLZ945 or anti-CSF-1. Most cells that expressed CCL2 and CCR2 were monocytes/moDCs, which suggests a model whereby monocytes that infiltrate the CNS produce CCL2, thus amplifying inflammation by further recruitment of CCR2-expressing cells. Given that CSF-1R signaling in monocytes/macrophages induces CCL2 expression [35-37], this suggests that its blockade reduces CNS inflammation by two mechanisms: 1) by reducing numbers of cells that produce CCL2, and 2) by reducing CCL2 production of surviving cells, which together amounts to greatly diminished CCL2 levels in the CNS during EAE. This is consistent with an essential role of CCL2 and CCR2 in EAE, since interventions that affect them attenuate disease [65-67]. It is also possible that in addition to monocytes, reduced CCL2 directly affects recruitment of $CCR2^+$ Th cells to the CNS, given a report that CCR2 drives their recruitment to the CNS [65]. Together with our result showing reduced GM-CSF and IL-1β production in the CNS, it is likely that CSF-1R inhibition suppresses EAE by depleting CCL2- and IL-1β-expressing APCs; IL-1β has an essential role in EAE [6, 31, 68, 69] by acting on $CD4^+$ T cells to promote their proliferation and GM-CSF production; GM-CSF is also essential to EAE development by acting on monocytes to induce their pro-inflammatory phenotype and IL-1β production, thus completing a positive feedback loop that sustains inflammation in EAE [70]. Inhibiting CSF-1R signaling would therefore interrupt this pro-inflammatory feedback loop, resulting in the sustained EAE suppression we observed upon treatment with BLZ945 and anti-CSF-1 MAb.

MAb therapies against CSF-1 and small molecule inhibitors of CSF-1R have been tested in multiple clinical trials and disease contexts, including autoimmune and oncological settings [71-76]. These trials have demonstrated that blockade of CSF-1/CSF-1R is well tolerated by patients [75, 77, 78]. Targeting CSF-1/CSF-1R in MS has not been tested, but agents used in preexisting trials would likely be suitable for testing in MS. Moreover, because CSF-1R signaling is not required by myeloid progenitors residing in the BM or CNS (for microglia) [29, 56], the effects of these treatments would be reversible. Indeed, there is complete repopulation of microglia within one week after cessation of treatment with CSF-1R inhibitors [29]. A treatment modality can be envisioned whereby blocking CSF-1R signaling for therapy of MS would follow an intermittent regimen, given for a period of time, instead of as a continuous treatment. Thus, as a potential therapy that depletes pathogenic myeloid cells in MS, targeting CSF-1/CSF-1R offers several potential advantages, including the potential of being readily translatable to clinical testing.

In conclusion, our findings show that blocking CSF-1R signaling dramatically decreases EAE severity by reducing number of inflammatory APCs in the CNS. Anti-CSF-1 MAb treatments have an advantage over BLZ945 treatments, and likely other small molecule inhibitors of CSF-1R function, in that they preferentially deplete inflammatory microglia, while sparing quiescent microglia and their homeostatic functions. This limited depletion, however, does not diminish the therapeutic effect of anti-CSF1 MAb treatment compared to BLZ945 treatment. Reducing CSF-1R signaling via neutralization of CSF-1 seems, therefore, to be a promising therapeutic strategy for MS therapy.

MATERIALS AND METHODS

Mice

All mice used in this study were on C57BL/6J genetic background. Mice were either obtained from The Jackson Laboratories (Bar Harbor, Maine) or bred in-house. All experimental procedures were approved by the Institutional Animal Care and Use Committee of Thomas Jefferson University.

Flow Cytometry

Isolated cells were stimulated with PMA (500 ng/mL; Sigma Aldrich), ionomycin (50 ng/mL; Sigma Aldrich), and 1 µL/mL Golgiplug (BD Biosciences) for 4 h at 37^{o}C. After stimulation, cells were washed with PBS containing 3% FBS (v/v). Cell surface antigens were stained with Abs in 100 µL of PBS/3% FBS for 20-30 min at 4^{o}C. Cells were then washed and fixed with 100 µL Fix and Perm Medium A (Thermo Fisher) for 20 min at room temperature and washed again. Cells were permeabilized with Fix and Perm Medium B (Thermo Fisher) and stained with Abs against intracellular antigens in 100 µL Fix and Perm Medium B and 100 µL PBS/3%FBS for 1 h. Cells were then washed twice, resuspended in 500 µL PBS and analyzed on a BD FACSAria Fusion flow cytometer (BD Biosciences).

Induction and Scoring of EAE

EAE was induced by immunization with 1:1 emulsion of PBS and complete Freund's adjuvant (CFA) containing 5 mg/mL heat killed *M. tuberculosis* (BD Biosciences) and 1 mg/mL MOG_{35-55} peptide (Genscript). Mice were immunized on the both flanks by subcutaneous injection of the emulsion for a total of 200 µL. Pertussis toxin was i.p. injected on days 0 and 2 post-immunization at 200 ng per dose. Mice were scored according to the following scale: 0 - No clinical symptoms. 0.5 - Partial paralysis of the tail or waddling gait. 1.0 - Full paralysis of the tail. 1.5 - Full paralysis of the tail and waddling gait. 2.0 - Partial paralysis in one leg. 2.5 - Partial paralysis in both legs or one leg paralyzed. 3.0 - Both legs paralyzed. 3.5 - Ascending paralysis. 4.0 - Paralysis above the hips. 4.5 – Moribund; mouse being unable to right itself for 30 seconds. 5.0 - Death.

448 **Isolation of Immune Cells from the CNS**

449 Mice were anesthetized and blood was removed by perfusion with 60 mL PBS. Spinal cord was flushed out of
450 the spinal column with PBS. Brains and spinal cords were pooled and cut manually into small pieces in 700 µL
451 Liberase TL dissolved in RPMI at 0.7 mg/mL (Roche) then incubated at 37ºC for 30 min before reaction was
452 quenched using complete media containing FBS. Tissue was homogenized by pushing through a 100 µm sterile
453 filter with syringe plunger. Homogenate was centrifuged at 1500 RPM (300 x g) for 5 min and resuspended in
454 25 mL of 70% 1x Percoll-PBS (90% Percoll, 10% 10x PBS). 25 mL of 30% Percoll-PBS was gently overlayed
455 onto the 70% layer and was centrifuged at 2000 RPM without brake at room temperature for 30 min. Cells that
456 pooled at the interface of 30/70% layers and the majority of the 30% layer were then collected, diluted with PBS
457 or media and centrifuged at 1500 RPM (300 x g) for 5 min.

458

459

460 **Antibody Titer Measurement**

461 Serum was collected from peripheral blood of animals treated with Rat IgG_{2A} (Clone: 2A3; Bio X Cell), anti-CSF1
462 MAb (Clone: 5A1; Bio X Cell), anti-CSF-1R MAb (Clone: AFS98; Bio X Cell), anti-IL-34 MAb (Clone: 780310,
463 Novus Biologicals). 96-well ELISA plates were coated with the same MAb that was used to treat animals
464 overnight at room temperature and blocked with 1% BSA for 2 h. Plates were washed and incubated with serum
465 for 1 h and washed. Anti-Mouse IgG-HRP conjugate secondary Ab (Jackson Immunolabs) was used to detect
466 the presence of anti-Rat IgG response by measuring absorbance at 450 nm and subtracting absorbance at 540
467 nm.

468

469 **BLZ945 Preparation and Treatment**

470 BLZ945 (Selleck Chemicals and MedChemExpress) was prepared from powder in 20% captisol at 12 mg/mL.
471 Mice were treated with BLZ945 by oral gavage with 4-6 mg/treatment/day. In initial experiments, we used BLZ945
472 prepared in 20% captisol, and 20% captisol as control, which were a generous gift from Novartis International
473 AG.

474

475

In vivo CSF-1, Anti-CSF-1, Anti-IL-34, and Anti-CSF-1R Treatments

Recombinant CSF-1 (4 µg/dose; R&D Systems) was given to EAE mice on days 4, 8, 12, 16 post immunization (p.i.) by intraperitoneal (i.p.) injection. All MAb treatments were also given by i.p. injection. Prophylactic treatments with anti-CSF-1 (200 µg/dose; clone: 5A1; Bio X Cell) started on day 0 p.i. and were given every other day until disease onset when dosing was changed to every day. In therapeutic treatments, MAb was given every day, starting on days indicated in figures, for the duration of acute phase of the disease (typically days 11-25 p.i.), then switched to every other day for the rest of the experiments. Equal amounts of control IgG1 (Clone: HPRN; Bio X Cell) were used to treat control mice. Mice were treated with anti-IL-34 MAb (100 µg/dose; Clone: 780310; Novus Biologicals) every other day for the duration of the experiment. Anti-CSF-1R Mab (400 µg/dose; Clone: AFS98; Bio X Cell) was given every other day. In experiments with anti-IL-34 and anti-CSF-1R MAbs, equal amounts of control IgG2A (Clone: 2A3; Bio X Cell) were given to control mice.

Bone Marrow-Derived DC Culture

Bone marrow (BM) was isolated from tibia and femurs of mice and BM cells were cultured at 1 x 10^6 cells per mL in a total volume of 10 mL in petri dishes with GM-CSF (20 ng/mL) + IL-4 (20 ng/mL) for 4 days. On the 4^{th} day, 5 mL of media was removed from the plates, cells were pelleted by centrifugation and resuspended in 5 mL fresh media containing GM-CSF and IL-4. The cell suspension was added back to the original petri dishes and cultured for an additional 3 days. To induce a mature DC phenotype, cells were washed, replated in fresh media containing LPS (300 ng/mL) and cultured for 72 h. For cultures involving monocytes, $CD11b^+$ cells were isolated from BM cell suspension of $CD45.1^+$ mice by MACS positive selection (Miltenyi Biotec) and then $Ly6C^{Hi}Ly6G^-$ monocytes were sorted on a FACSAria Fusion instrument (BD Biosciences). Isolated monocytes were then added to $CD45.2^+$ total BM cell cultures.

Co-culture of DCs and T cells and Proliferation Assay

For proliferation assays, 4 x 10^4 DCs were co-cultured with 1.6 x 10^5 2D2 $CD4^+$ T cells in 96-well U-bottom tissue culture plates. Cells were stimulated with MOG_{35-55} peptide (25 µg/mL) for 72 h. At approximately 60 h after starting the culture, 1 µCi of [^{3}H]Thymidine (Perkin-Elmer) was added to each well in a volume of 50 µL. Cells were harvested 24 h later and counts per minute (C.P.M.) measured in MicroBeta2 beta counter (Perkin-Elmer).

Library Preparation and RNA-seq Analyses

Next-generation sequencing libraries were prepared using the Illumina TruSeq Stranded Total RNA library preparation kit, with high quality RNA (RIN >= 8.7) and 200 ng of input RNA. Libraries were assessed for quality using the PerkinElmer Labchip GX and qPCR using the Kapa Library Quantification Kit and the Life Technologies Viia7 Real-time PCR instrument. Libraries were diluted to 2 nM and sequenced in a paired-end (2 x 100bp), dual-indexed format on the Illumina HiSeq2500 using the High Output v4 chemistry.

RNA-seq reads were demultiplexed into sample-specific fastq files and aligned to the mm10 reference genome using the DRAGEN genome pipeline [79] to produce BAM files. Generated BAM files were read into R statistical computing environment and gene counts were obtained using the Rsubread package, producing a feature/gene counts matrix. Differential expression analysis was performed using the R/Bioconductor package DESeq2 which uses a negative binomial model [80]. Analysis was performed using standard thresholds and parameters while filtering genes with low mean normalized counts. Further downstream analysis was performed using the Ingenuity Pathway Analysis (IPA) and GSEA software using the normalized read count table. Additionally, differentially expressed genes ($p<0.01$) were entered into the DAVID utility for functional annotation and analyzed for gene ontology terms for biological processes and for KEGG pathway terms [38, 39].

Author Contributions

Bogoljub Ciric and Daniel Hwang were responsible for the conceptualization of this project. Daniel Hwang was responsible carrying out experiments and analysis of data.

Larissa Lumi Watanabe Ishikawa, Alexandra Boehm, Ziver Sahin, Giacomo Casella, Soohwa Jang, and Maryamsadat Seyedsadr assisted in carrying out experiments.

Michael Gonzalez, James Garifallo and Hakon Hakonarson were responsible for RNA sequencing experiments and assisted with analysis of RNA sequencing data.

Guang-Xian Zhang and Abdolmohamad Rostami assisted with manuscript preparation and provided helpful insights in interpreting data.

Acknowledgments

We thank Katherine Regan for editing the manuscript.

Funding

This work was supported by a grant from the National Multiple Sclerosis Society (RG-1803-30491) to B. Ciric.

REFERENCES

1. Pyonteck, S.M., et al., *CSF-1R inhibition alters macrophage polarization and blocks glioma progression.* Nat Med, 2013. **19**(10): p. 1264-72. PMC3840724 PMID: 24056773.
2. Lassmann, H. and M. Bradl, *Multiple sclerosis: experimental models and reality.* Acta Neuropathol, 2017. **133**(2): p. 223-244. PMC5250666 PMID: 27766432.
3. Ramaglia, V., et al., *Multiplexed imaging of immune cells in staged multiple sclerosis lesions by mass cytometry.* Elife, 2019. **8**. PMC6707785 PMID: 31368890.
4. Zrzavy, T., et al., *Loss of 'homeostatic' microglia and patterns of their activation in active multiple sclerosis.* Brain, 2017. **140**(7): p. 1900-1913. PMC6057548 PMID: 28541408.
5. Machado-Santos, J., et al., *The compartmentalized inflammatory response in the multiple sclerosis brain is composed of tissue-resident CD8+ T lymphocytes and B cells.* Brain, 2018. **141**(7): p. 2066-2082. PMC6022681 PMID: 29873694.
6. Croxford, A.L., et al., *The Cytokine GM-CSF Drives the Inflammatory Signature of CCR2+ Monocytes and Licenses Autoimmunity.* Immunity, 2015. **43**(3): p. 502-14. PMID: 26341401.
7. Fife, B.T., et al., *CC chemokine receptor 2 is critical for induction of experimental autoimmune encephalomyelitis.* J Exp Med, 2000. **192**(6): p. 899-905. PMC2193286 PMID: 10993920.
8. Giles, D.A., et al., *CNS-resident classical DCs play a critical role in CNS autoimmune disease.* J Clin Invest, 2018. **128**(12): p. 5322-5334. PMC6264723 PMID: 30226829.
9. Percin, G.I., et al., *CSF1R regulates the dendritic cell pool size in adult mice via embryo-derived tissue-resident macrophages.* Nat Commun, 2018. **9**(1): p. 5279. PMC6290072 PMID: 30538245.
10. Hume, D.A. and K.P. MacDonald, *Therapeutic applications of macrophage colony-stimulating factor-1 (CSF-1) and antagonists of CSF-1 receptor (CSF-1R) signaling.* Blood, 2012. **119**(8): p. 1810-20. PMID: 22186992.
11. MacDonald, K.P., et al., *The colony-stimulating factor 1 receptor is expressed on dendritic cells during differentiation and regulates their expansion.* J Immunol, 2005. **175**(3): p. 1399-405. PMID: 16034075.
12. Crespo, O., et al., *Tyrosine kinase inhibitors ameliorate autoimmune encephalomyelitis in a mouse model of multiple sclerosis.* J Clin Immunol, 2011. **31**(6): p. 1010-20. PMC3225802 PMID: 21847523.
13. Nissen, J.C., et al., *Csf1R inhibition attenuates experimental autoimmune encephalomyelitis and promotes recovery.* Exp Neurol, 2018. **307**: p. 24-36. PMID: 29803827.
14. Freskgard, P.O. and E. Urich, *Antibody therapies in CNS diseases.* Neuropharmacology, 2017. **120**: p. 38-55. PMID: 26972827.
15. Chitu, V., et al., *Emerging Roles for CSF-1 Receptor and its Ligands in the Nervous System.* Trends Neurosci, 2016. **39**(6): p. 378-393. PMC4884457 PMID: 27083478.
16. Wang, Y. and M. Colonna, *Interkeukin-34, a cytokine crucial for the differentiation and maintenance of tissue resident macrophages and Langerhans cells.* Eur J Immunol, 2014. **44**(6): p. 1575-81. PMC4137395 PMID: 24737461.
17. Sarahrudi, K., et al., *Elevated levels of macrophage colony-stimulating factor in human fracture healing.* J Orthop Res, 2010. **28**(5): p. 671-6. PMID: 19950360.
18. Aharinejad, S., et al., *Elevated CSF1 serum concentration predicts poor overall survival in women with early breast cancer.* Endocr Relat Cancer, 2013. **20**(6): p. 777-83. PMID: 24016870.
19. Hamilton, J.A., *Colony-stimulating factors in inflammation and autoimmunity.* Nat Rev Immunol, 2008. **8**(7): p. 533-44. PMID: 18551128.
20. Kawano, Y., et al., *Measurement of serum levels of macrophage colony-stimulating factor (M-CSF) in patients with uremia.* Exp Hematol, 1993. **21**(2): p. 220-3. PMID: 8425560.
21. Moon, S.J., et al., *Increased levels of interleukin 34 in serum and synovial fluid are associated with rheumatoid factor and anticyclic citrullinated peptide antibody titers in patients with rheumatoid arthritis.* J Rheumatol, 2013. **40**(11): p. 1842-9. PMID: 23996288.
22. Chang, E.J., et al., *IL-34 is associated with obesity, chronic inflammation, and insulin resistance.* J Clin Endocrinol Metab, 2014. **99**(7): p. E1263-71. PMID: 24712570.
23. Wang, H., J. Cao, and X. Lai, *Serum Interleukin-34 Levels Are Elevated in Patients with Systemic Lupus Erythematosus.* Molecules, 2016. **22**(1). PMID: 28036035.
24. Luo, J., et al., *Colony-stimulating factor 1 receptor (CSF1R) signaling in injured neurons facilitates protection and survival.* J Exp Med, 2013. **210**(1): p. 157-72. PMC3549715 PMID: 23296467.

25. Wang, Y., et al., *Nonredundant roles of keratinocyte-derived IL-34 and neutrophil-derived CSF1 in Langerhans cell renewal in the steady state and during inflammation.* Eur J Immunol, 2016. **46**(3): p. 552-9. PMC5658206 PMID: 26634935.
26. Okubo, M., et al., *Macrophage-Colony Stimulating Factor Derived from Injured Primary Afferent Induces Proliferation of Spinal Microglia and Neuropathic Pain in Rats.* PLoS One, 2016. **11**(4): p. e0153375. PMC4829214 PMID: 27071004.
27. Erblich, B., et al., *Absence of colony stimulation factor-1 receptor results in loss of microglia, disrupted brain development and olfactory deficits.* PLoS One, 2011. **6**(10): p. e26317. PMC3203114 PMID: 22046273.
28. Sierra, A., et al., *Microglia derived from aging mice exhibit an altered inflammatory profile.* Glia, 2007. **55**(4): p. 412-24. PMID: 17203473.
29. Elmore, M.R., et al., *Colony-stimulating factor 1 receptor signaling is necessary for microglia viability, unmasking a microglia progenitor cell in the adult brain.* Neuron, 2014. **82**(2): p. 380-97. PMC4161285 PMID: 24742461.
30. Hawley, C.A., et al., *Csf1r-mApple Transgene Expression and Ligand Binding In Vivo Reveal Dynamics of CSF1R Expression within the Mononuclear Phagocyte System.* J Immunol, 2018. **200**(6): p. 2209-2223. PMC5834790 PMID: 29440354.
31. Lin, C.C. and B.T. Edelson, *New Insights into the Role of IL-1beta in Experimental Autoimmune Encephalomyelitis and Multiple Sclerosis.* J Immunol, 2017. **198**(12): p. 4553-4560. PMC5509030 PMID: 28583987.
32. Lutz, M.B., et al., *GM-CSF Monocyte-Derived Cells and Langerhans Cells As Part of the Dendritic Cell Family.* Front Immunol, 2017. **8**: p. 1388. PMC5660299 PMID: 29109731.
33. Mildner, A., et al., *CCR2+Ly-6Chi monocytes are crucial for the effector phase of autoimmunity in the central nervous system.* Brain, 2009. **132**(Pt 9): p. 2487-500. PMID: 19531531.
34. Mahad, D., et al., *Modulating CCR2 and CCL2 at the blood-brain barrier: relevance for multiple sclerosis pathogenesis.* Brain, 2006. **129**(Pt 1): p. 212-23. PMID: 16230319.
35. Sierra-Filardi, E., et al., *CCL2 shapes macrophage polarization by GM-CSF and M-CSF: identification of CCL2/CCR2-dependent gene expression profile.* J Immunol, 2014. **192**(8): p. 3858-67. PMID: 24639350.
36. Stutchfield, B.M., et al., *CSF1 Restores Innate Immunity After Liver Injury in Mice and Serum Levels Indicate Outcomes of Patients With Acute Liver Failure.* Gastroenterology, 2015. **149**(7): p. 1896-1909 e14. PMC4672154 PMID: 26344055.
37. Tagliani, E., et al., *Coordinate regulation of tissue macrophage and dendritic cell population dynamics by CSF-1.* J Exp Med, 2011. **208**(9): p. 1901-16. PMC3171096 PMID: 21825019.
38. Huang da, W., B.T. Sherman, and R.A. Lempicki, *Systematic and integrative analysis of large gene lists using DAVID bioinformatics resources.* Nat Protoc, 2009. **4**(1): p. 44-57. PMID: 19131956.
39. Huang da, W., B.T. Sherman, and R.A. Lempicki, *Bioinformatics enrichment tools: paths toward the comprehensive functional analysis of large gene lists.* Nucleic Acids Res, 2009. **37**(1): p. 1-13. PMC2615629 PMID: 19033363.
40. Hemmings, B.A. and D.F. Restuccia, *PI3K-PKB/Akt pathway.* Cold Spring Harb Perspect Biol, 2012. **4**(9): p. a011189. PMC3428770 PMID: 22952397.
41. Rietkotter, E., et al., *Anti-CSF-1 treatment is effective to prevent carcinoma invasion induced by monocyte-derived cells but scarcely by microglia.* Oncotarget, 2015. **6**(17): p. 15482-93. PMC4558165 PMID: 26098772.
42. Fleetwood, A.J., et al., *Granulocyte-macrophage colony-stimulating factor (CSF) and macrophage CSF-dependent macrophage phenotypes display differences in cytokine profiles and transcription factor activities: implications for CSF blockade in inflammation.* J Immunol, 2007. **178**(8): p. 5245-52. PMID: 17404308.
43. Sierra-Filardi, E., et al., *Activin A skews macrophage polarization by promoting a proinflammatory phenotype and inhibiting the acquisition of anti-inflammatory macrophage markers.* Blood, 2011. **117**(19): p. 5092-101. PMID: 21389328.
44. Verreck, F.A., et al., *Human IL-23-producing type 1 macrophages promote but IL-10-producing type 2 macrophages subvert immunity to (myco)bacteria.* Proc Natl Acad Sci U S A, 2004. **101**(13): p. 4560-5. PMC384786 PMID: 15070757.
45. Komohara, Y., et al., *Possible involvement of the M2 anti-inflammatory macrophage phenotype in growth of human gliomas.* J Pathol, 2008. **216**(1): p. 15-24. PMID: 18553315.
46. Foucher, E.D., et al., *IL-34 induces the differentiation of human monocytes into immunosuppressive macrophages. antagonistic effects of GM-CSF and IFNgamma.* PLoS One, 2013. **8**(2): p. e56045. PMC3568045 PMID: 23409120.

47. Smith, A.M., et al., *M-CSF increases proliferation and phagocytosis while modulating receptor and transcription factor expression in adult human microglia.* J Neuroinflammation, 2013. **10**: p. 85. PMC3729740 PMID: 23866312.
48. Guan, Y., et al., *Antigen presenting cells treated in vitro by macrophage colony-stimulating factor and autoantigen protect mice from autoimmunity.* J Neuroimmunol, 2007. **192**(1-2): p. 68-78. PMC2743086 PMID: 18006080.
49. MacDonald, K.P., et al., *An antibody against the colony-stimulating factor 1 receptor depletes the resident subset of monocytes and tissue- and tumor-associated macrophages but does not inhibit inflammation.* Blood, 2010. **116**(19): p. 3955-63. PMID: 20682855.
50. Hamilton, J.A. and A. Achuthan, *Colony stimulating factors and myeloid cell biology in health and disease.* Trends Immunol, 2013. **34**(2): p. 81-9. PMID: 23000011.
51. Djelloul, M., et al., *RAE-1 expression is induced during experimental autoimmune encephalomyelitis and is correlated with microglia cell proliferation.* Brain Behav Immun, 2016. **58**: p. 209-217. PMID: 27444966.
52. Smith, A.M., et al., *Adult human glia, pericytes and meningeal fibroblasts respond similarly to IFNy but not to TGFbeta1 or M-CSF.* PLoS One, 2013. **8**(12): p. e80463. PMC3855168 PMID: 24339874.
53. Caescu, C.I., et al., *Colony stimulating factor-1 receptor signaling networks inhibit mouse macrophage inflammatory responses by induction of microRNA-21.* Blood, 2015. **125**(8): p. e1-13. PMC4335087 PMID: 25573988.
54. De, I., et al., *CSF1 overexpression has pleiotropic effects on microglia in vivo.* Glia, 2014. **62**(12): p. 1955-67. PMC4205273 PMID: 25042473.
55. Wei, S., et al., *Functional overlap but differential expression of CSF-1 and IL-34 in their CSF-1 receptor-mediated regulation of myeloid cells.* J Leukoc Biol, 2010. **88**(3): p. 495-505. 2924605 PMID: 20504948.
56. Stanley, E.R. and V. Chitu, *CSF-1 receptor signaling in myeloid cells.* Cold Spring Harb Perspect Biol, 2014. **6**(6). PMC4031967 PMID: 24890514.
57. Brizzi, M.F., et al., *Regulation of c-kit expression in human myeloid cells.* Stem Cells, 1993. **11 Suppl 2**: p. 42-8. PMID: 7691327.
58. Kusmartsev, S. and D.I. Gabrilovich, *Effect of tumor-derived cytokines and growth factors on differentiation and immune suppressive features of myeloid cells in cancer.* Cancer Metastasis Rev, 2006. **25**(3): p. 323-31. PMC1693571 PMID: 16983515.
59. Berardi, A.C., et al., *Basic fibroblast growth factor mediates its effects on committed myeloid progenitors by direct action and has no effect on hematopoietic stem cells.* Blood, 1995. **86**(6): p. 2123-9. PMID: 7662960.
60. Heo, S.K., et al., *Targeting c-KIT (CD117) by dasatinib and radotinib promotes acute myeloid leukemia cell death.* Sci Rep, 2017. **7**(1): p. 15278. PMC5681687 PMID: 29127384.
61. Qin, H., et al., *FGFR1OP2-FGFR1 induced myeloid leukemia and T-cell lymphoma in a mouse model.* Haematologica, 2016. **101**(3): p. e91-4. PMC4815735 PMID: 26589915.
62. Zhao, L., P. Ye, and T.J. Gonda, *The MYB proto-oncogene suppresses monocytic differentiation of acute myeloid leukemia cells via transcriptional activation of its target gene GFI1.* Oncogene, 2014. **33**(35): p. 4442-9. PMID: 24121275.
63. Demoulin, J.B. and C.P. Montano-Almendras, *Platelet-derived growth factors and their receptors in normal and malignant hematopoiesis.* Am J Blood Res, 2012. **2**(1): p. 44-56. PMC3301440 PMID: 22432087.
64. Song, G., Y. Li, and G. Jiang, *Role of VEGF/VEGFR in the pathogenesis of leukemias and as treatment targets (Review).* Oncol Rep, 2012. **28**(6): p. 1935-44. PMID: 22993103.
65. Kara, E.E., et al., *CCR2 defines in vivo development and homing of IL-23-driven GM-CSF-producing Th17 cells.* Nat Commun, 2015. **6**: p. 8644. PMC4639903 PMID: 26511769.
66. Huang, D.R., et al., *Absence of monocyte chemoattractant protein 1 in mice leads to decreased local macrophage recruitment and antigen-specific T helper cell type 1 immune response in experimental autoimmune encephalomyelitis.* J Exp Med, 2001. **193**(6): p. 713-26. PMC2193420 PMID: 11257138.
67. Chu, H.X., et al., *Role of CCR2 in inflammatory conditions of the central nervous system.* J Cereb Blood Flow Metab, 2014. **34**(9): p. 1425-9. PMC4158674 PMID: 24984897.
68. McGinley, A.M., et al., *Interleukin-17A Serves a Priming Role in Autoimmunity by Recruiting IL-1beta-Producing Myeloid Cells that Promote Pathogenic T Cells.* Immunity, 2020. **52**(2): p. 342-356 e6. PMID: 32023490.

69. Komuczki, J., et al., *Fate-Mapping of GM-CSF Expression Identifies a Discrete Subset of Inflammation-Driving T Helper Cells Regulated by Cytokines IL-23 and IL-1beta.* Immunity, 2019. **50**(5): p. 1289-1304 e6. PMID: 31079916.
70. Pare, A., et al., *IL-1beta enables CNS access to CCR2(hi) monocytes and the generation of pathogenic cells through GM-CSF released by CNS endothelial cells.* Proc Natl Acad Sci U S A, 2018. **115**(6): p. E1194-E1203. PMC5819409 PMID: 29358392.
71. Novartis Pharmaceuticals. *MCS110 in Patients With Pigmented Villonodular Synovitis (PVNS) or Giant Cell Tumor of the Tendon Sheath (GCTTS)*. 2012 [cited 2015 12/29/2015]; Available from: https://clinicaltrials.gov/ct2/show/NCT01643850.
72. Novartis Pharmaceuticals. *Efficacy Study of MCS110 Given With Carboplatin and Gemcitabine in Advanced Triple Negative Breast Cancer (TNBC)*. 2015 [cited 2015 12/29/2015]; Available from: https://clinicaltrials.gov/ct2/show/NCT02435680.
73. Novartis Pharmaceuticals. *A Phase I/II Open-label Study of MCS110 in Patients With Prostate Cancer and Bone Metastases*. 2008 [cited 2015 12/29/2015]; Available from: https://clinicaltrials.gov/ct2/show/NCT00757757.
74. Company, E.L.a. *A Study of IMC-CS4 in Subjects With Advanced Solid Tumors*. 2011 [cited 2015 12/29/2015]; Available from: https://clinicaltrials.gov/ct2/show/NCT01346358.
75. Cassier, P.A., et al., *CSF1R inhibition with emactuzumab in locally advanced diffuse-type tenosynovial giant cell tumours of the soft tissue: a dose-escalation and dose-expansion phase 1 study.* Lancet Oncol, 2015. **16**(8): p. 949-56. PMID: 26179200.
76. Genovese, M.C., et al., *Results from a Phase IIA Parallel Group Study of JNJ-40346527, an Oral CSF-1R Inhibitor, in Patients with Active Rheumatoid Arthritis despite Disease-modifying Antirheumatic Drug Therapy.* J Rheumatol, 2015. **42**(10): p. 1752-60. PMID: 26233509.
77. Butowski, N., et al., *Orally administered colony stimulating factor 1 receptor inhibitor PLX3397 in recurrent glioblastoma: an Ivy Foundation Early Phase Clinical Trials Consortium phase II study.* Neuro Oncol, 2016. **18**(4): p. 557-64. PMC4799682 PMID: 26449250.
78. Tap, W.D., et al., *Structure-Guided Blockade of CSF1R Kinase in Tenosynovial Giant-Cell Tumor.* N Engl J Med, 2015. **373**(5): p. 428-37. PMID: 26222558.
79. Goyal, A., et al., *Ultra-Fast Next Generation Human Genome Sequencing Data Processing Using DRAGEN Bio-IT Processor for Precision Medicine.* Open Journal of Genetics, 2017. **Vol. 7**(No. 1). PMID.
80. Love, M.I., W. Huber, and S. Anders, *Moderated estimation of fold change and dispersion for RNA-seq data with DESeq2.* Genome Biol, 2014. **15**(12): p. 550. PMC4302049 PMID: 25516281.

FIGURES

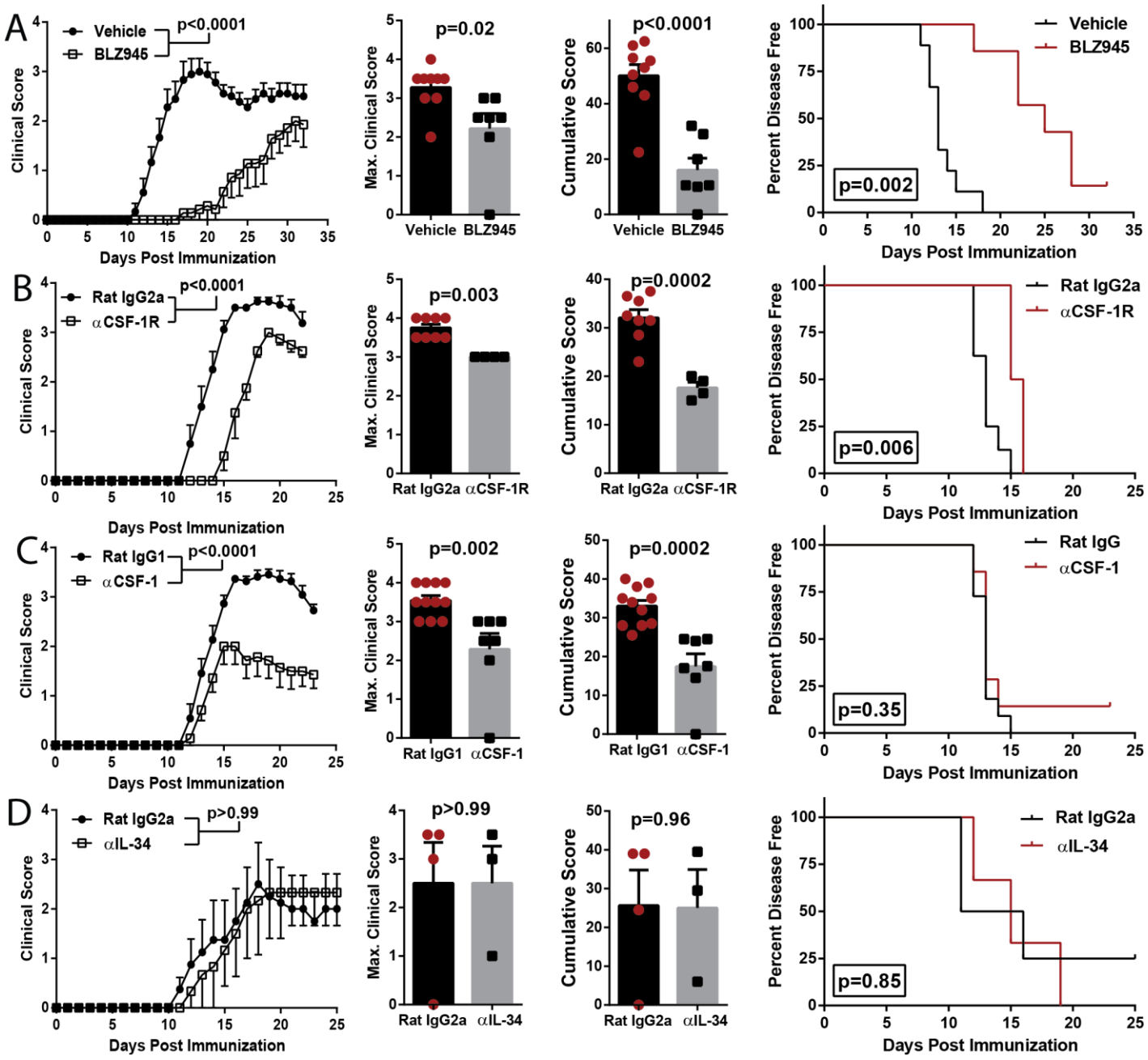

Figure 1: Blocking CSF-1R activity suppresses EAE. A-D) C57BL/6J mice were immunized with MOG_{35-55} for EAE induction. Clinical course, maximum and cumulative clinical scores, and Kaplan-Meier plots depicting percent of disease-free animals over time are shown. Significance for clinical course data was calculated by two-way repeated measures ANOVA. Significance for maximum and cumulative clinical scores was calculated by Student's *t*-test. Error bars are S.E.M. Significance for Kaplan-Meier plots was calculated by comparing disease-free curves with the log-rank (Mantel-Cox) test. **A)** EAE animals treated orally with BLZ945 (n=9; 4 mg/day [1]) or vehicle (n=7; 20% Captisol) daily, starting from day of immunization. Data were compiled from two independent experiments. **B)** Treatment with anti-CSF-1R MAb (n=4) or control rat IgG2a (n=8). MAbs were i.p. injected every other day (400 µg per dose). **C)** Treatment with anti-CSF-1 MAb (n=7) or control rat IgG1 (n=11). MAbs were i.p. injected every other day (200 µg per dose). Data were compiled from two independent experiments. **D)** Treatment with anti-IL-34 MAb (n=3) or control rat IgG2a MAb (n=4). MAbs were i.p. injected every other day (100 µg per dose).

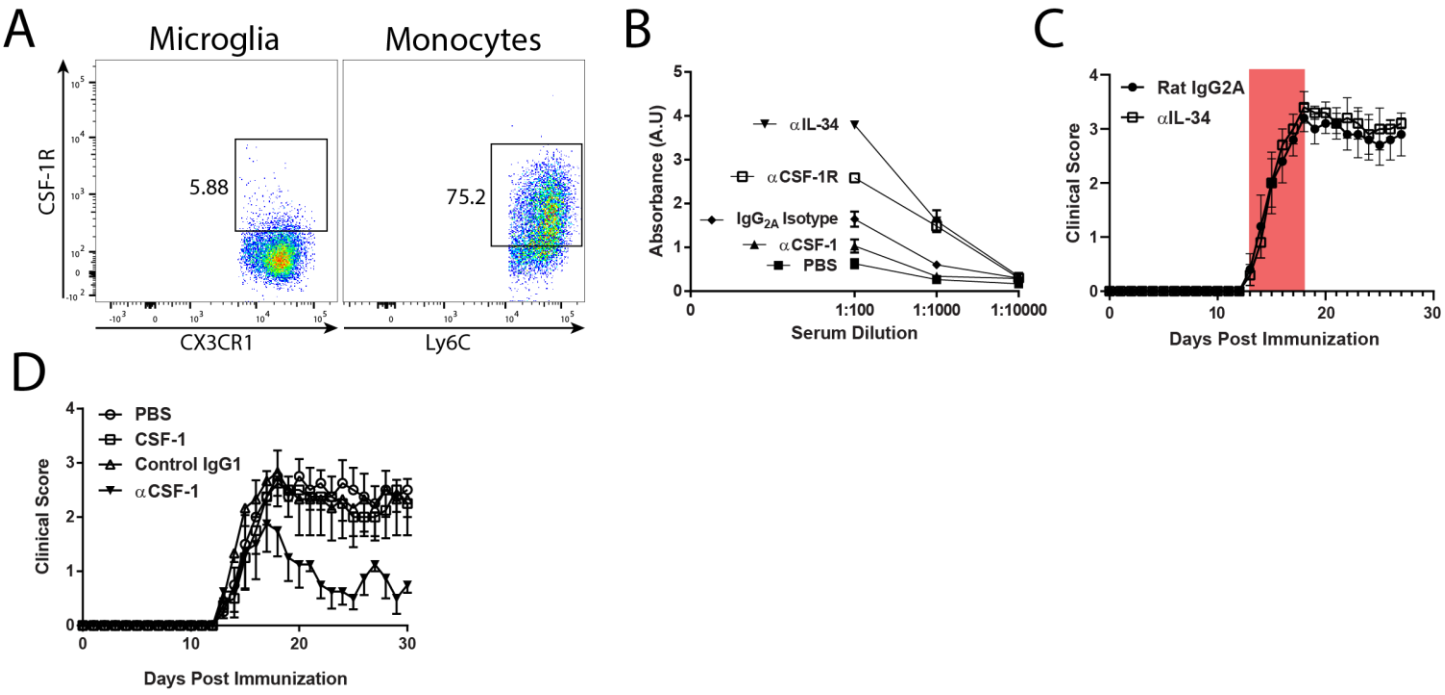

Supplemental Figure 1: A) C57BL6/J mice were immunized with MOG_{35-55} and treated with anti-CSF1 MAb (200 µg, every other day), control rat IgG1 MAb (200 µg, every other day), recombinant mouse CSF-1 (4 µg per dose, given on days 4, 8 ,12 ,16 p.i.) or PBS by i.p. injection. **B)** Serum Ab titers of mice with EAE treated with MAbs against IL-34 (n=3), CSF-1R (n=3), IgG2a isotype (n=4), CSF1 (n=3), and control animals treated with PBS (n=6). Error bars are standard error from the mean. **C)** Flow cytometry plots depicting staining of $CD45^{+}CD11b^{+}CX3CR1^{Hi}$ microglia and $CD45^{Hi}CD11b^{+}Ly6G^{-}Ly6C^{Hi}$ monocytes for CSF-1R with the AFS98 MAb. **D)** C57BL6/J mice were immunized with MOG_{35-55} and treated with anti-IL-34 Mab (55 µg per day, i.p) for the period indicated by the red box.

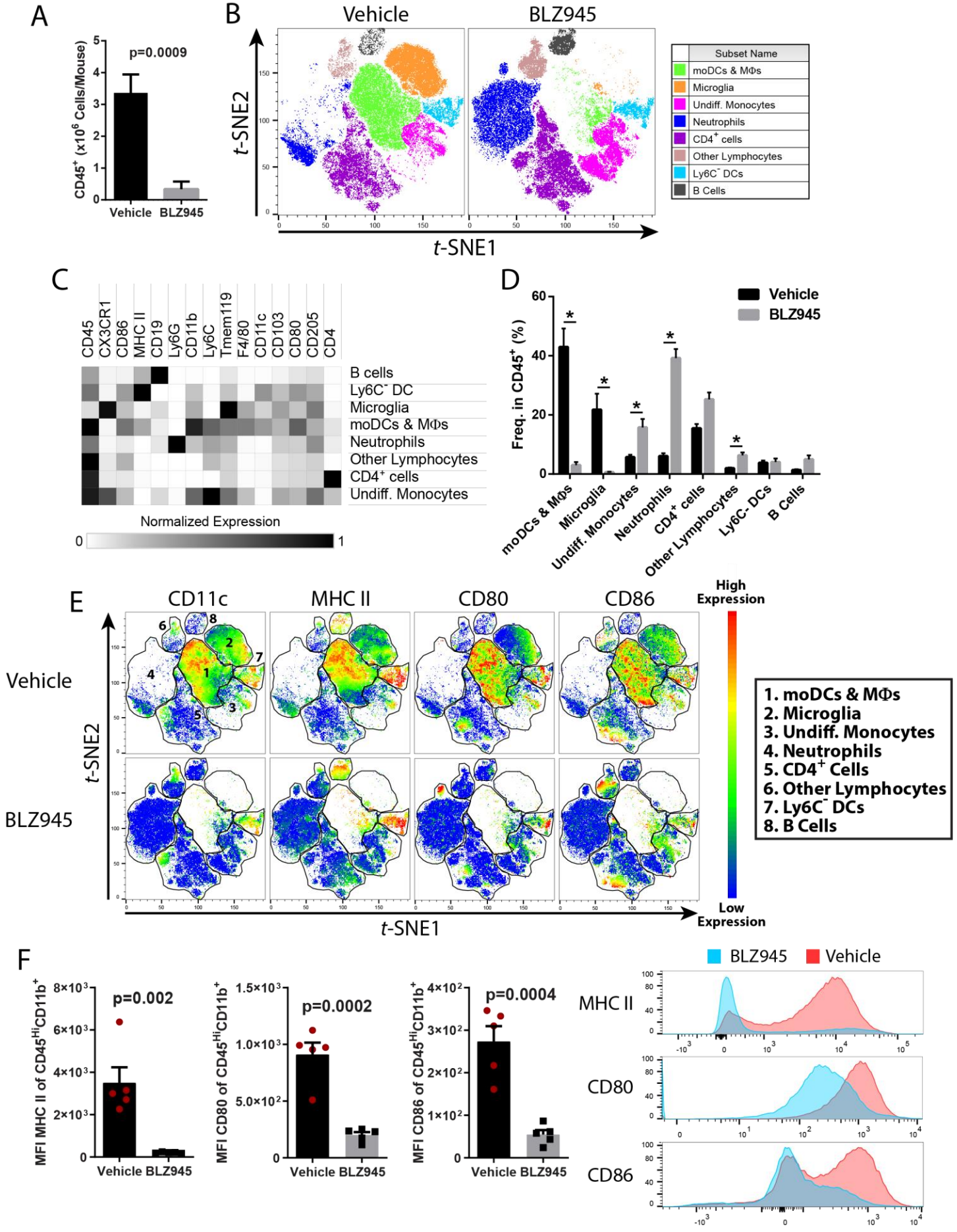

766

Figure 2: CSF-1R inhibition depletes myeloid APCs in the CNS of mice with EAE. C57BL/6J mice were immunized with MOG_{35-55} for EAE induction and treated orally with BLZ945 (4 mg/day) or vehicle control (20% captisol) daily, starting on the day of immunization. Mice were sacrificed on day 15 p.i., and brain and spinal cords were pooled for cell isolation. **A)** Numbers of CNS $CD45^+$ cells (n=7/group, combined from two independent experiments). **B)** *t*-SNE plot depicting clustering of $CD45^+$ cells (n=5 mice per group). moDCs and macrophages were defined by their expression of CD11b, CD11c, MHC II, CD80 and CD86. Microglia were defined as $CD45^+CD11b^+Tmem119^+CX3CR1^{Hi}$ cells. Undifferentiated monocytes were defined as $CD45^{Hi}Ly6C^{Hi}CD11c^-$ cells that were overall MHC $II^{Lo/Neg}$. Neutrophils were defined as $CD45^+CD11b^+Ly6G^{Hi}$. $CD4^+$ cells were defined as $CD45^+CD4^+$. Other lymphocytes were defined as $CD45^{Hi}SSC^{Lo}$. $Ly6C^-$ DCs were defined as $CD45^{Hi}CD11b^+CD11c^+MHCII^{Hi}Ly6C^-$ cells. B cells were defined as $CD45^+CD19^+$. **C)** Heatmap showing normalized expression of markers used to identify clusters. **D)** Quantification of clusters between vehicle and BLZ945-treated mice with EAE. **E)** Heat map of CD11c, MHC II, CD80 and CD86 expression among $CD45^+$ cells. **F)** MFI of MHC II, CD80 and CD86 among $CD45^{Hi}CD11b^+$ myeloid cells. Representative histograms showing fluorescence intensity of MHC II, CD80 and CD86 between vehicle- and BLZ945-treated animals is also shown. Y-axis is frequency of cells as normalized to mode. Significance was calculated with Student's t test. For D),* indicates a p-value less than 0.02. Error bars are S.E.M.

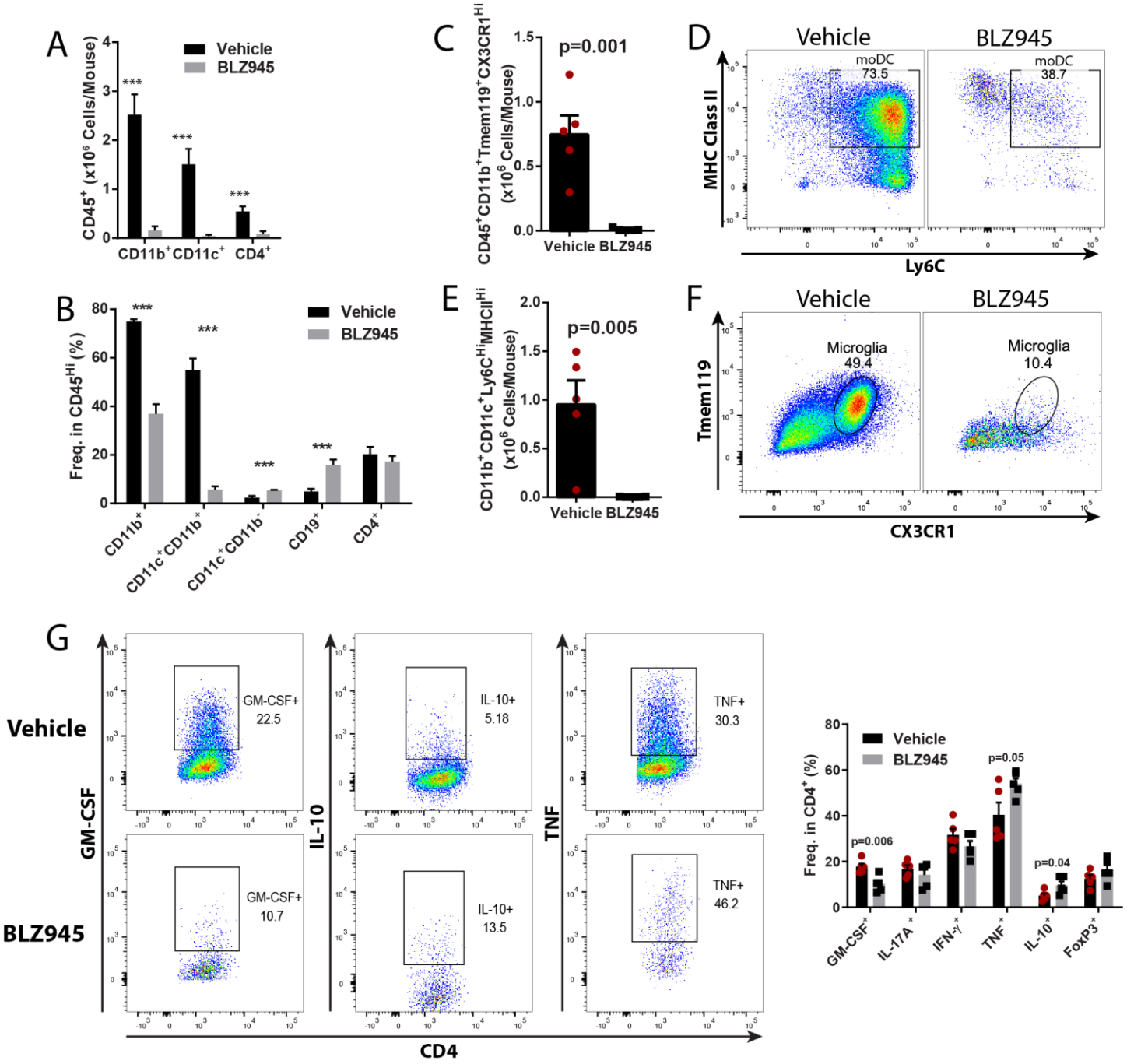

Supplementary Figure 2: Inhibition of CSF-1R signaling alters both myeloid and T cell compartments in the CNS of EAE mice. C57BL/6J mice were immunized with MOG_{35-55} for EAE induction and treated orally with BLZ945 (200 mg/kg/day) or vehicle control (20% captisol) daily, starting on the day of immunization. Mice were sacrificed on day 15 p.i., and pooled brain and spinal cords of each mouse were used for cell isolation (n=5/group). **A)** Numbers of $CD11b^+$, $CD11c^+$ and $CD4^+$ cells. **B)** Frequency of $CD11b^+$, $CD11b^+CD11c^+$ $CD11b^+CD11c^-$, $CD19^+$, and $CD4^+$ cells in $CD45^{Hi}$ cells. **C-F)** Numbers of $CD45^+CD11b^+Tmem119^+CX3CR1^{Hi}$ microglia and $CD45^{Hi}CD11b^+Ly6C^{Hi}$ $MHCII^{Hi}$ moDCs. **G)** Quantification of GM-CSF, IL-17A, IFN-γ, TNF, IL-10 and FoxP3 expression by $CD4^+$ cells from the CNS. Significance was calculated with Student's t test. Error bars are S.E.M.

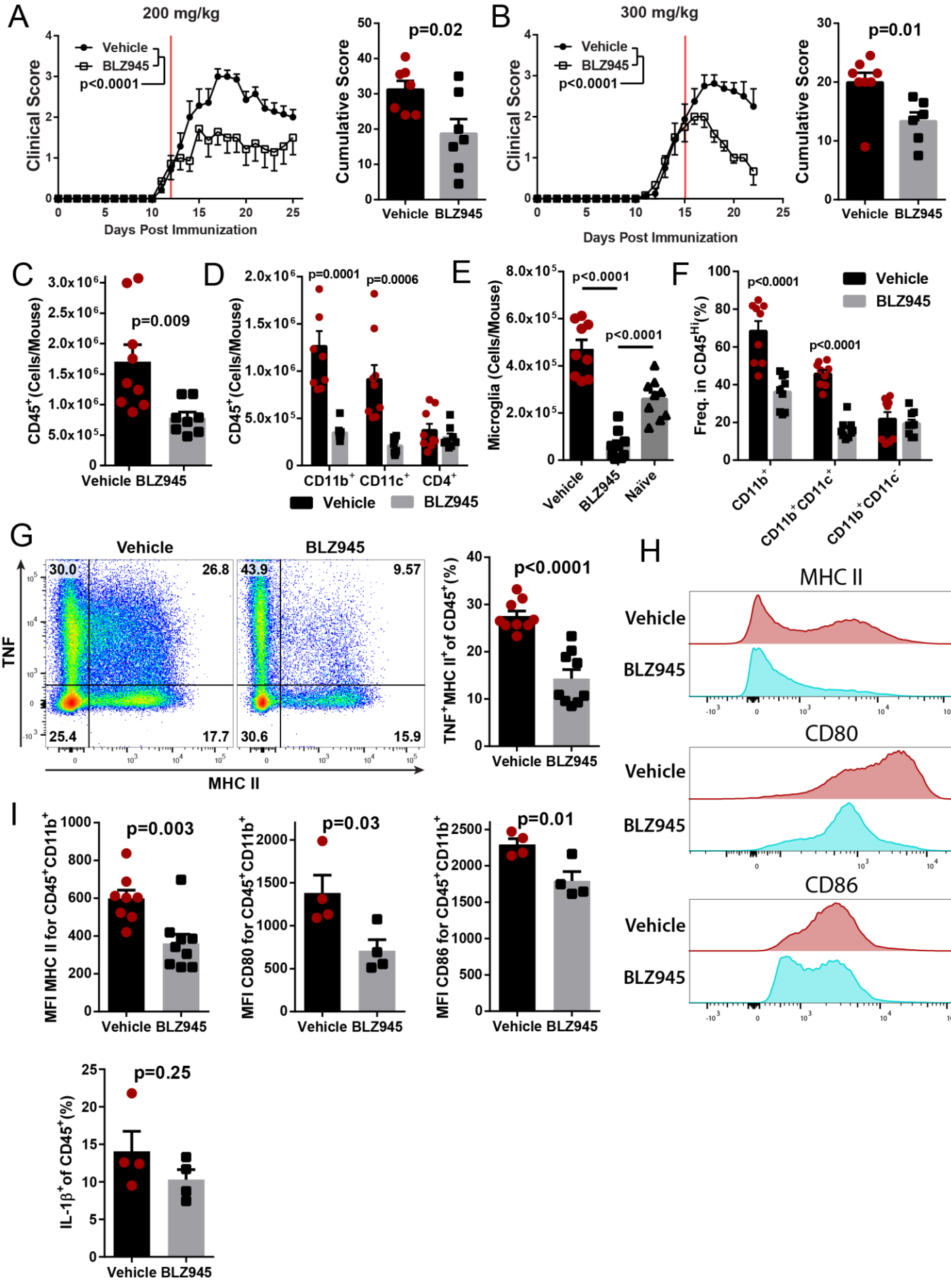

Figure 3. BLZ945 suppresses ongoing clinical EAE, and reduces the number of myeloid APCs in the CNS. C57BL/6J mice were immunized and allowed to develop clinical signs of EAE before treatment with BLZ945 (n=7) or vehicle (n=8). Treatments were given once per day by oral gavage. **A)** Clinical course and cumulative score for mice treated with 200 mg/kg BLZ945 starting at a clinical score of ~1. Red line indicates start of treatment. **B)** Mice treated with 300 mg/kg BLZ945 (n=6) or vehicle (n=8), starting at a clinical score of ~2. A) and B) were compiled from two independent experiments. Significance for clinical course determined by two-way repeated measures ANOVA, and by unpaired Student's t-test for cumulative scores. **C-I)** Analysis of the CNS (pooled brain and spinal cords) by flow cytometry. **C)** Number of $CD45^{+}$ cells. **D)** Number of $CD45^{+}$ cells that also expressed CD11b, CD11c, or CD4. **E)** Number of $CD45^{Lo}CD11b^{+}CX3CR1^{Hi}$ microglia. Naïve mice are untreated WT C57BL/6J mice that were not immunized or otherwise manipulated. **F)** Frequency of $CD45^{Hi}$ cells that also express CD11b and/or CD11c. **G)** TNF and MHC II expression in $CD45^{+}$ cells. **H-I)** Expression of MHC II, CD80 and CD86 in $CD45^{+}CD11b^{+}$ cells. Significance for C-I was calculated by unpaired Student's t test. P-value corrections for multiple comparisons was performed by false discovery rate approach with Q=0.01 as a cutoff. Error bars are S.E.M.

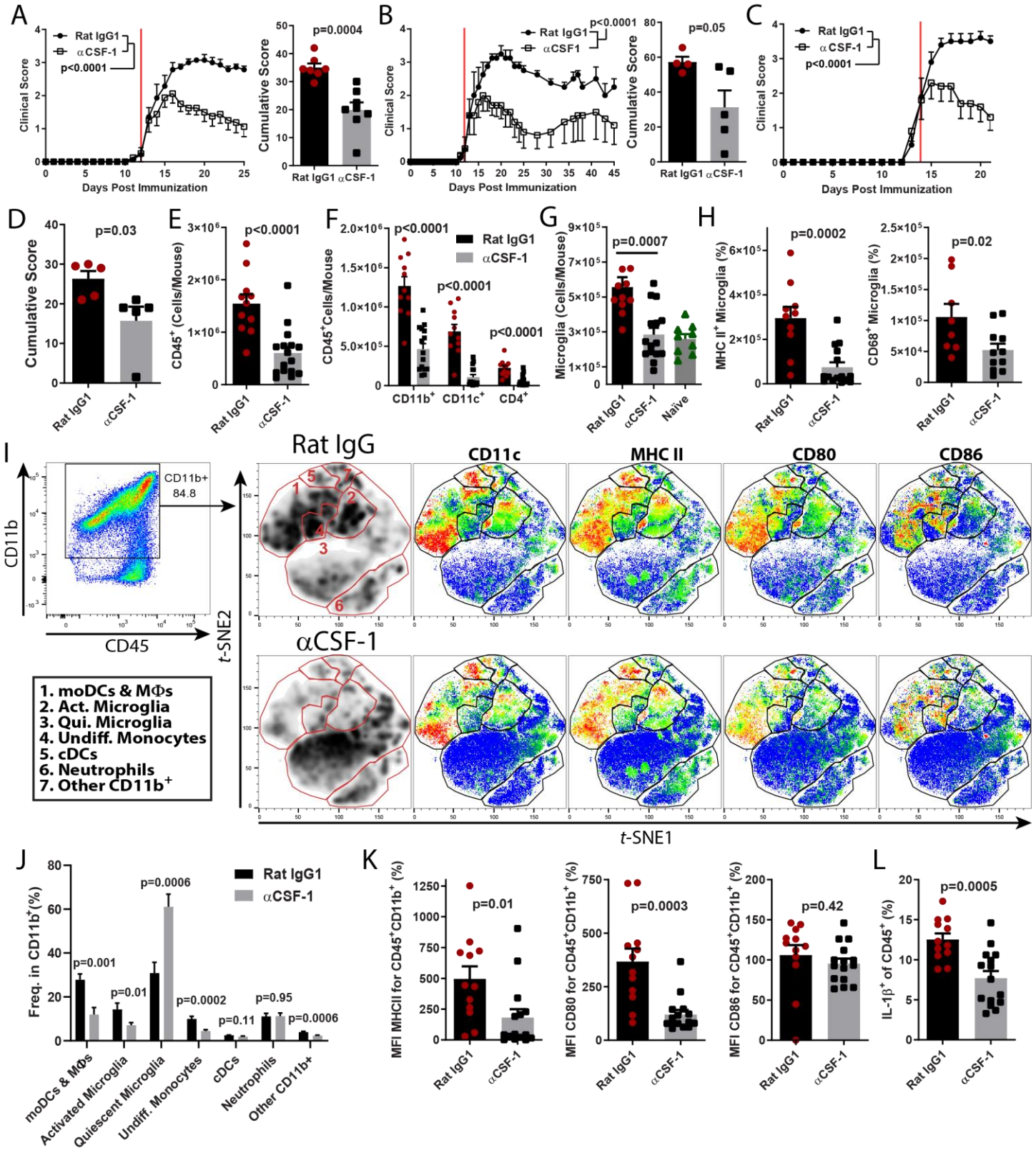

Figure 4: CSF-1 controls the population size of inflammatory myeloid cells in the CNS during EAE. A) Clinical course and cumulative score of mice with EAE treated with αCSF-1 MAb starting after disease onset (n=7 per group; compiled from 2 independent experiments). Red line denotes day that treatment was started. Mice were treated with 200 μg MAb per day. **B)** Clinical course and cumulative scores of mice treated long term with αCSF-1 MAb. Mice were treated daily until day 25, and then every other day for the duration of the experiment. **C-D)** Clinical course and cumulative score for mice treated with αCSF-1 MAb, starting at clinical score of 2.0 (n=4-5 per group). **E-L)** Characterization of immune cells from the CNS of control MAb- and αCSF-1 MAb-treated mice. **E)** Number of $CD45^+$ cells. **F)** Numbers of $CD11b^+$, $CD11c^+$ and $CD4^+$ cells. **G)** Numbers of $CD45^+CD11b^+$ $CX3CR1^{Hi}Tmem119^+$ microglia in control-treated, αCSF-1 MAb-treated, and naïve mice. **H)** Numbers of MHC II^+ and $CD68^+$ microglia in control MAb- and αCSF-1 MAb-treated mice. **I)** *t*-SNE analysis of $CD45^+CD11b^+$ cells. moDCs and macrophages were defined by their expression of CD11b, CD11c, MHC II, CD80 and CD86. Activated microglia were defined as $CD45^+CD11b^+Tmem119^+CX3CR1^{Hi}MHCII^+CD68^{+/-}$ cells. Quiescent microglia were defined as $CD45^+CD11b^+Tmem119^+CX3CR1^{Hi}MHCII^-CD68^-$. Undifferentiated monocytes were defined as $CD45^{Hi}Ly6C^{Hi}CD11c^-$ cells that were overall MHC $II^{Lo/Neg}$. Neutrophils were defined as $CD45^+CD11b^+Ly6G^{Hi}$. $CD4^+$ cells were defined as $CD45^+CD4^+$. cDCs were defined as $CD45^{Hi}CD11b^+CD11c^+MHCII^{Hi}Ly6C^-CD26^+$ cells. Other $CD11b^+$ cells expressed CD11c and CX3CR1 but did not express markers for antigen presentation. **J)** Quantification of clusters from I). **K)** Median fluorescence intensity of MHC II, CD80 and CD86 in $CD45^+CD11b^+$ cells. **L)** Frequency of IL-$1\beta^+$ cells among $CD45^+$ cells. Significance was calculated with unpaired Student's t test. Error bars are S.E.M.

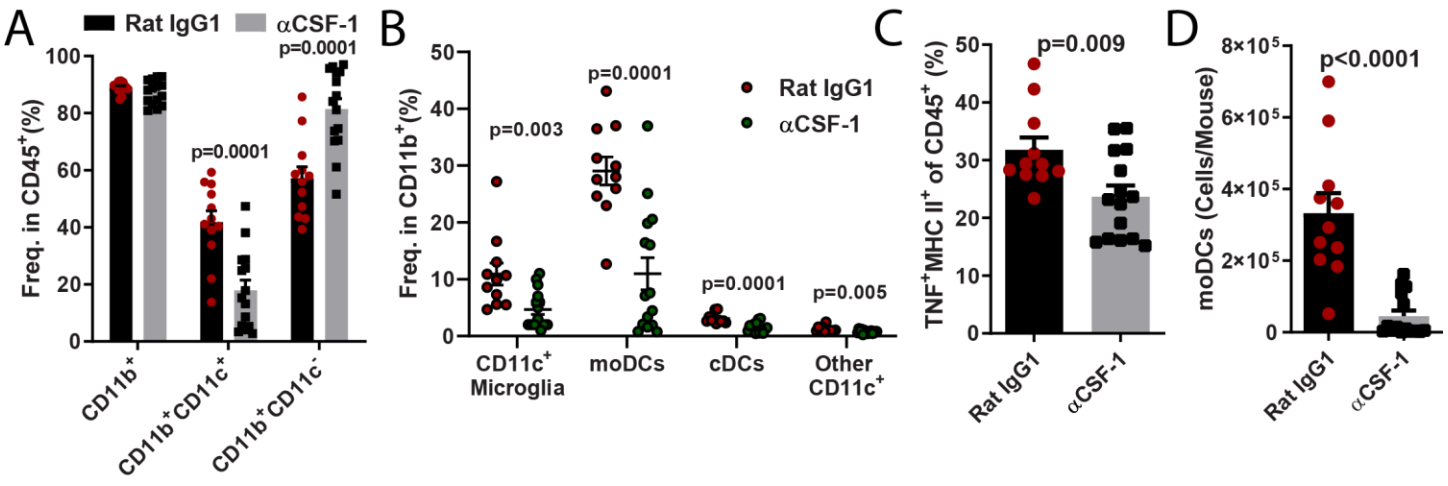

796

Supplementary Figure 3: Anti-CSF-1 treatment reduces numbers of DCs in the CNS of mice with EAE. A) Frequency of $CD11b^+$, $CD11b^+CD11c^+$, $CD11b^+CD11c^-$ cells among $CD45^+$ cells from the CNS of mice with EAE treated with either anti-CSF-1 or control MAb. **B)** Frequency of $CD11c^+$ microglia ($CD45^+CD11b^+CX3CR1^{Hi}Tmem119^+$), moDCs ($CD45^{Hi}CD11b^+$ $CD11c^+Ly6G^-Ly6C^{Hi}$MHC II^{Hi}), cDCs ($CD45^{Hi}CD11b^+CD11c^+CD26^+Ly6C^-MHCII^+$) and other $CD11c^+$ cells among $CD11b^+$ cells. **C)** Number of $CD45^{Hi}CD11b^+$ $CD11c^+Ly6G^-Ly6C^{Hi}$MHC II^{Hi} moDCs. **D)** Frequency of TNF^+MHC II^+ cells among $CD45^+$ cells. Significance was calculated with unpaired Student's t test. Error bars are S.E.M.

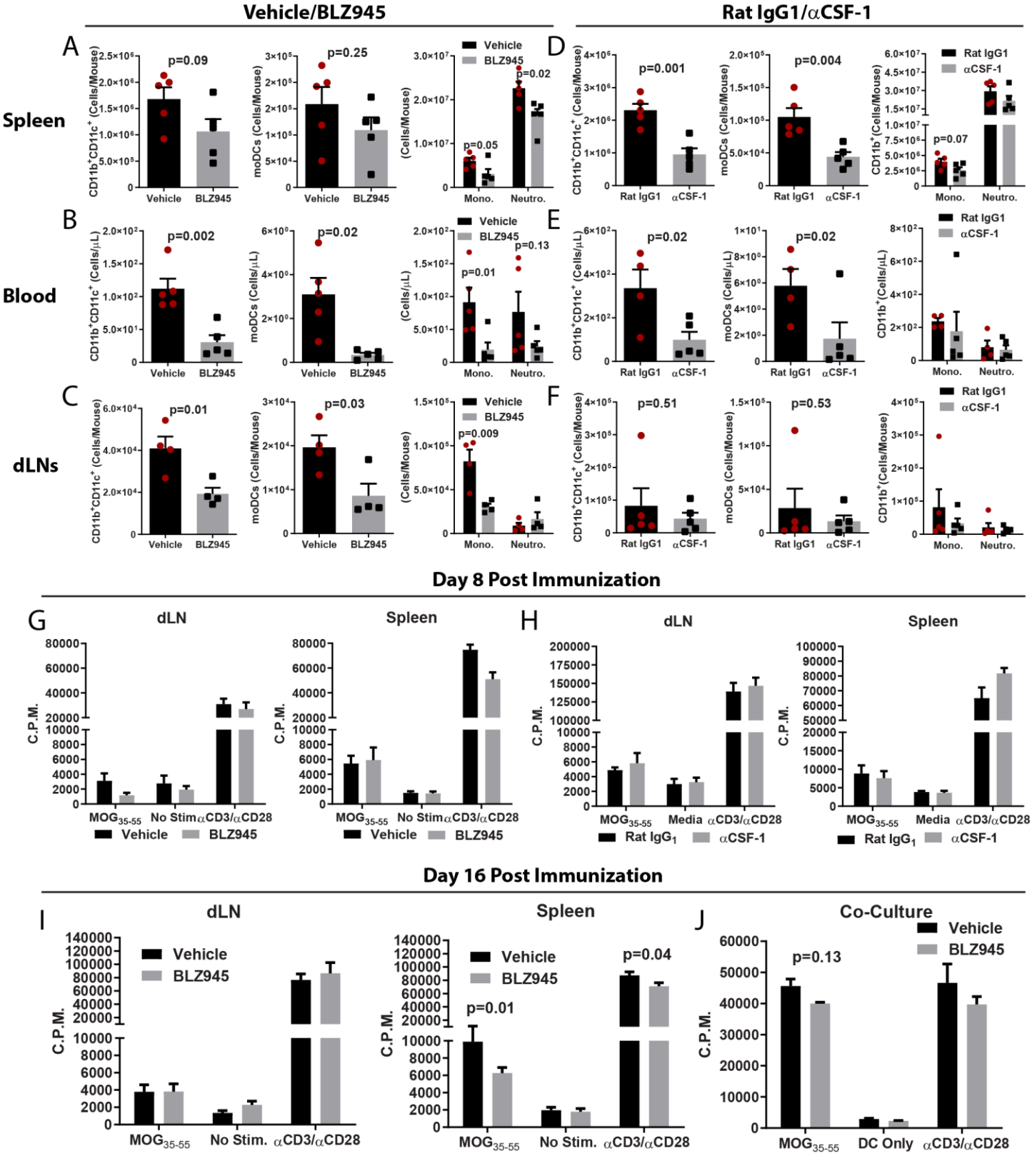

Figure 5: CSF-1R inhibition depletes myeloid DCs and monocytes in peripheral lymphoid compartments. Characterization of immune cells in the spleen, blood and dLNs from MOG_{35-55}-immunized mice sacrificed on day 8 p.i.. **A-C)** BLZ945- and vehicle-treated mice (n=5 per group). Numbers of $CD11b^+CD11c^+$, moDCs, monocytes and neutrophils in **A)** spleen, **B)** blood, and **C)** dLN. **E-F)** Same quantification as in A-C) but for anti-CSF-1- and rat IgG1 control MAbs-treated mice. **G)** [^{3}H]Thymidine proliferation assay for MOG_{35-55}-stimulated splenocytes and dLNs cells from BLZ945- and vehicle-treated mice harvested on day 8 p.i. **H)** Same analyses as in G), but for anti-CSF-1- and rat IgG1 control MAb-treated mice. **I)** [^{3}H]Thymidine proliferation assay for MOG_{35-55}-stimulated splenocytes and dLNs cells from BLZ945- and vehicle-treated mice harvested on day 16 p.i. **J)** $CD11c^+$ cells in splenocytes from BLZ945- and vehicle-treated mice harvested on day 8 p.i. $CD11c^+$ cells were isolated by magnetic bead sorting and mixed in a 1:10 ratio with $CD4^+$ T cells isolated from splenocytes of 2D2 mice, and stimulated with MOG_{35-55} for 72 h. Proliferation was then measured by [^{3}H]Thymidine incorporation assay. Statistical significance was calculated using two-way unpaired t test. Error bars are S.E.M.

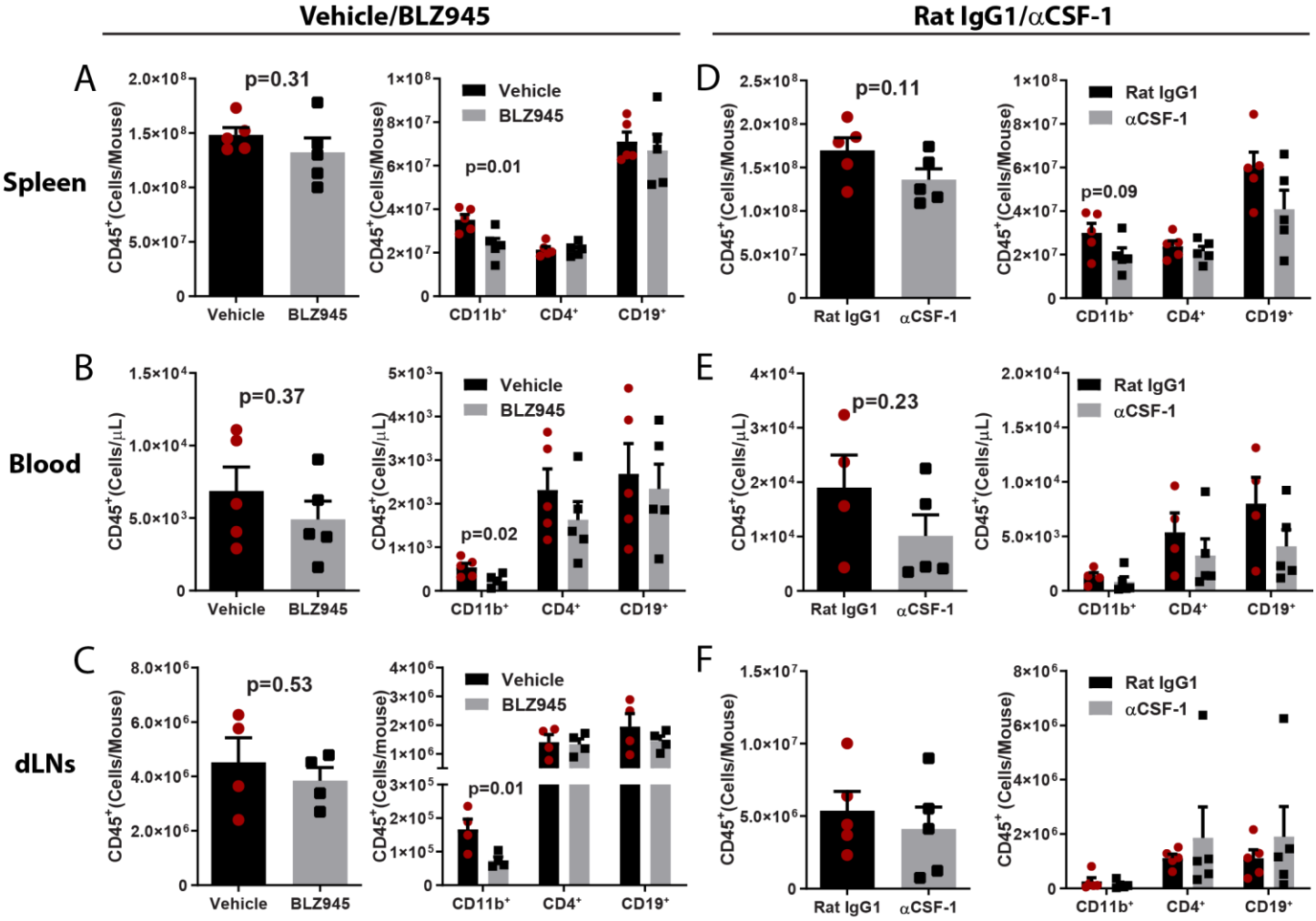

Supplementary Figure 4: Immune response in peripheral lymphoid organs of BLZ945- and Anti-CSF-1-treated mice on day 8 p.i. A-C) BLZ945- and vehicle-treated mice (n=5 per group). Number of $CD45^+$, $CD11b^+$, $CD4^+$ and $CD19^+$ cells in **A)** spleen, **B)** blood, and **C)** dLN. **E-F)** Same quantification as A-C) but for anti-CSF-1- and rat IgG1 control MAb-treated mice. Statistical significance was calculated using two-way unpaired t test. Error bars are standard S.E.M.

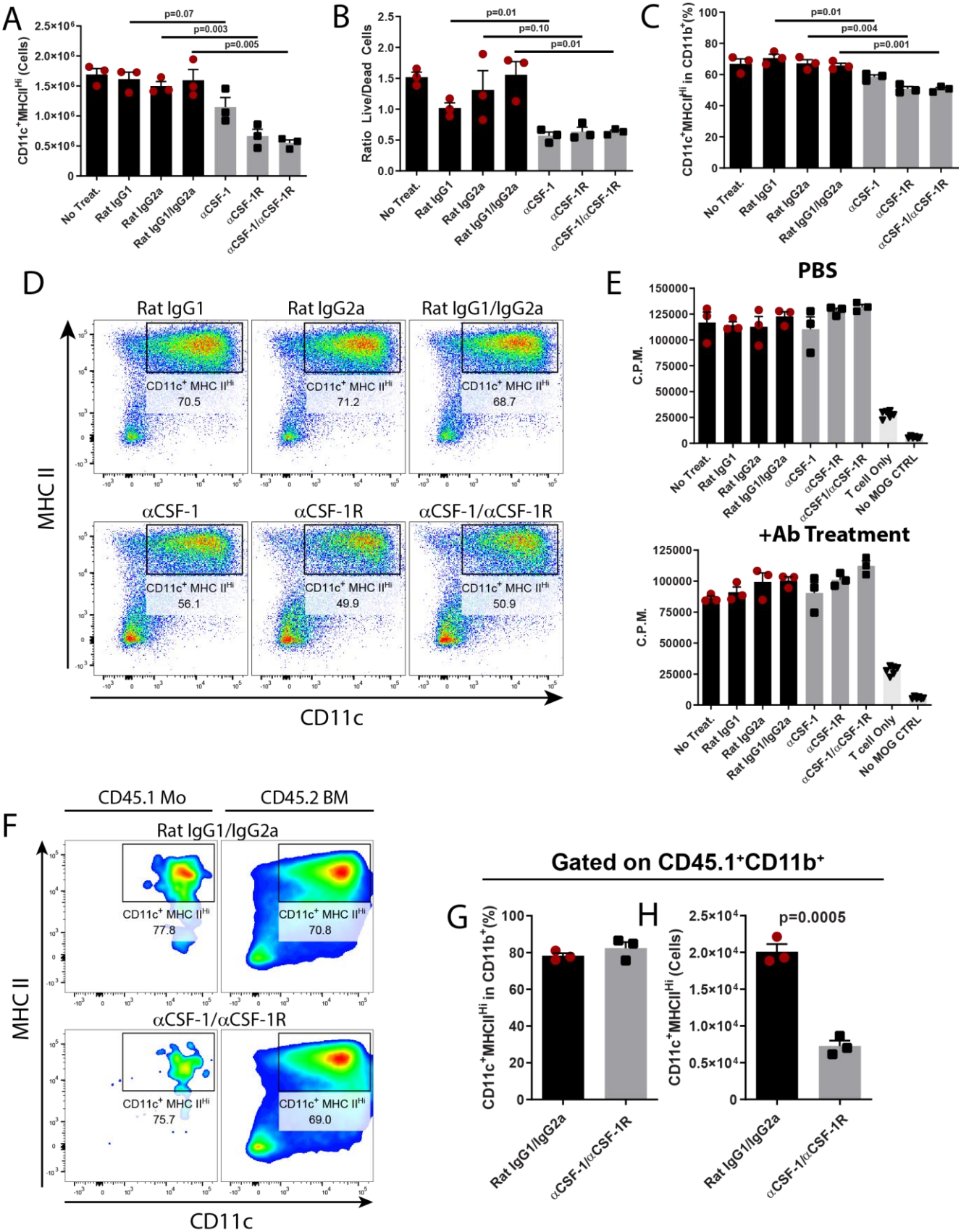

Figure 6: CSF-1R signaling promotes survival and proliferation of moDCs but not their APC function. BM cells were cultured in media supplemented with GM-CSF and IL-4 for 7 days in the presence of either control, or anti-CSF1 and anti-CSF-1R MAbs. BMDCs were then matured by stimulation with LPS for 24 h in the presence of the MAbs. **A)** Number of $CD11c^{+}MHCII^{Hi}$ cells in culture after GM-CSF + IL-4 treatment for 7 days. **B)** Ratio of Live/Dead cells after 24 h LPS treatment. **C-D)** Frequency of $CD11c^{+}MHCII^{Hi}$ cells after GM-CSF + IL-4 treatment for 7 days. **E)** Co-culture of LPS-matured BMDCs with $CD4^{+}$ T cells from 2D2 mice and MOG_{35-55} peptide (25 μg/mL). Co-cultures either did or did not contain control and neutralizing MAbs against CSF-1 and CSF-1R. Proliferation was measured using $[^{3}H]$Thymidine incorporation. C.P.M. = counts per minute. **F)** Monocytes were purified from the BM of CD45.1 mice and mixed with total BM of CD45.2 mice, then cultured as described above with control or anti-CSF1/anti-CSF-1R MAbs. Flow cytometry depicting CD11c and MHC II expression in $CD45.1^{+}CD11b^{+}$ and $CD45.2^{+}CD11b^{+}$ cells is shown. **G)** Frequency, and **H)** number of $CD11c^{+}MHC\ II^{Hi}$ cells among $CD45.1^{+}CD11b^{+}$ cells. Technical replicates for 1 of 2 independent experiments with similar results are shown. Statistical significance was calculated using two-way unpaired t test. Error bars are S.E.M.

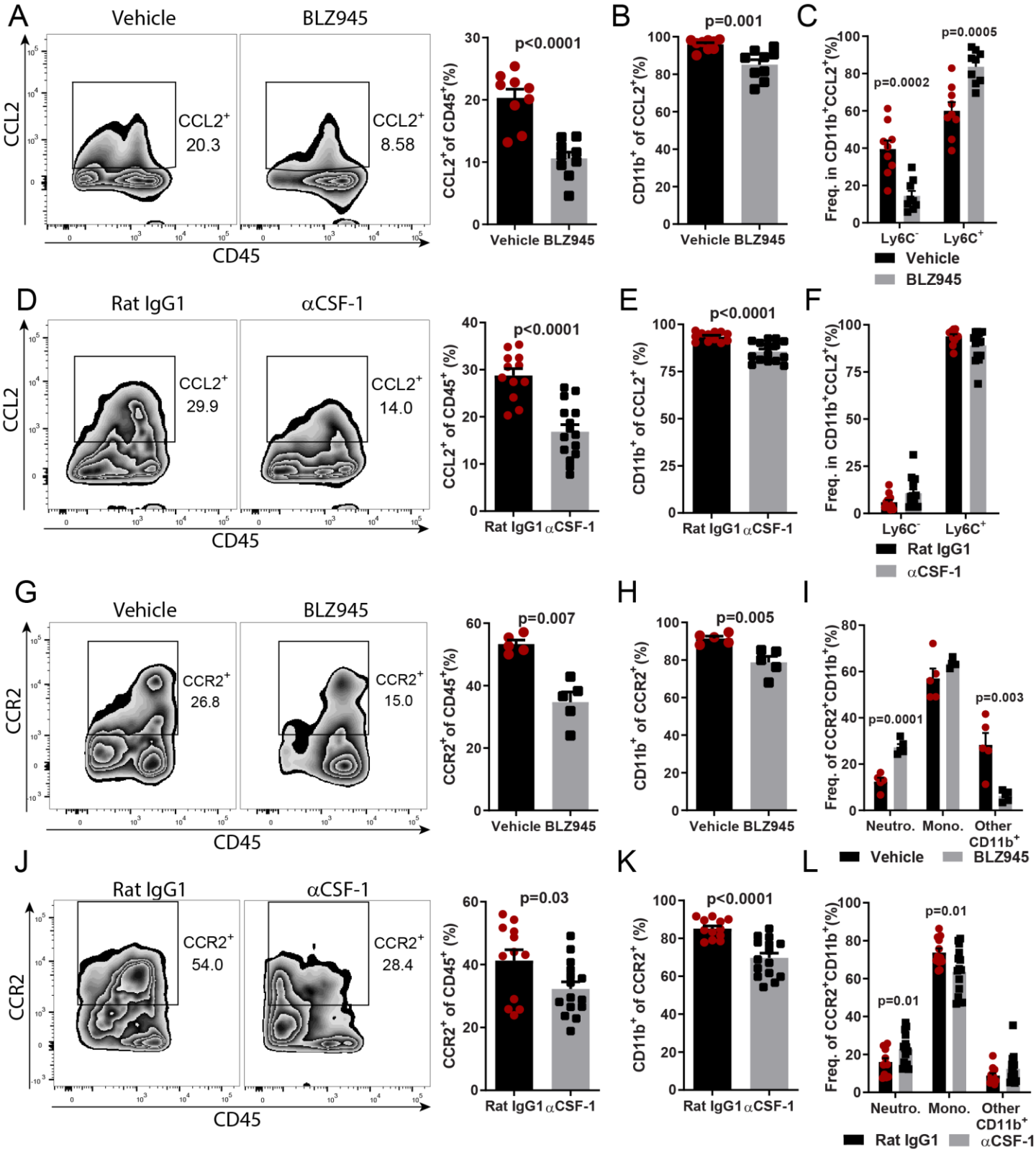

Figure 7: Blocking CSF-1R or CSF-1 reduces numbers of CCL2^{+} and CCR2^{+} myeloid cells in the CNS during EAE. A) Frequency of CCL2^{+} cells among CD45^{+} cells in the CNS of BLZ945- and vehicle-treated mice (n=9 per group) sacrificed after 6 days of treatment at day 20 p.i.. **B)** CD11b^{+} cells among CCL2^{+} cells. **C)** Frequency of Ly6C^{+} and Ly6C^{-} cells among CD11b^{+}CCL2^{+} cells. **D)** Frequency of CCL2^{+} cells among CD45^{+} cells from the CNS of anti-CSF-1- and control MAb-treated mice (n=12-15 per group), sacrificed after 6 days of treatment at 17 days p.i.. **E)** CD11b^{+} cells among CCL2^{+} cells. **F)** Frequency of Ly6C^{+} and Ly6C^{-} cells among CD11b^{+}CCL2^{+} cells. **G)** Frequency of CCR2^{+} cells among CD45^{+} cells from the CNS of BLZ945- and vehicle-treated mice from A). **H)** CD11b^{+} cells among CCL2^{+} cells. **I)** Frequency of neutrophils (CD45^{Hi}CD11b^{+}Ly6G^{Hi}Ly6C^{Int}), monocytes/monocyte-derived cells (CD45^{Hi}CD11b^{+}Ly6G$^{Neg/Lo}$Ly6C^{+}) and other CD11b^{+} cells among CCR2^{+}CD11b^{+} cells. **J)** Frequency of CCR2^{+} cells among CD45^{+} cells from the CNS of anti-CSF-1- and control MAb-treated mice from D). **K)** CD11b^{+} cells among CCL2^{+} cells. **L)** Frequency of neutrophils (CD45^{Hi}CD11b^{+}Ly6G^{Hi}Ly6C^{Int}), monocytes/monocyte-derived cells (CD45^{Hi}CD11b^{+}Ly6G$^{Neg/Lo}$Ly6C^{+}) and other CD11b^{+} cells among CCR2^{+}CD11b^{+} cells. Statistical significance was calculated using two-tailed unpaired t test. Error bars are S.E.M.

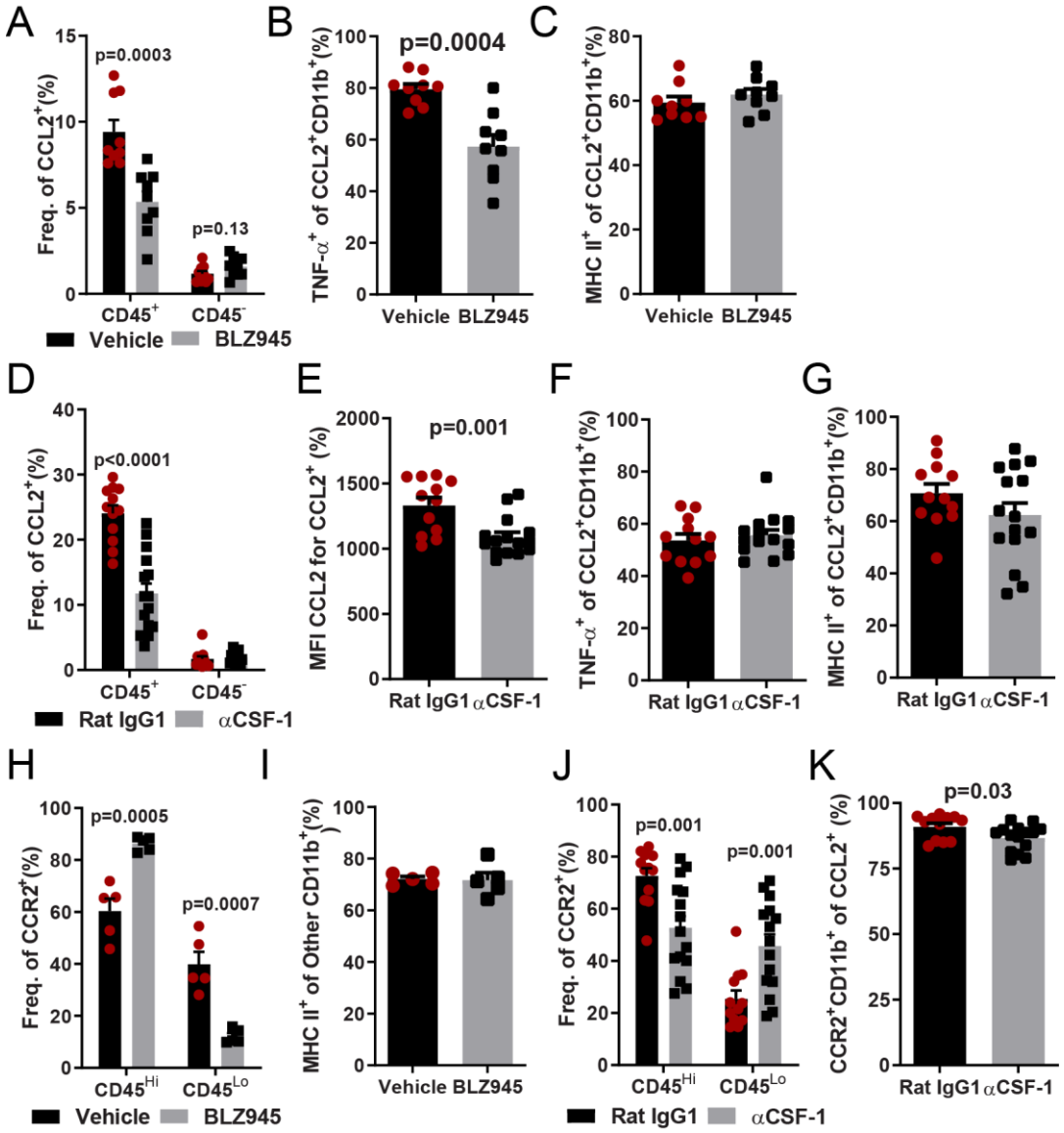

Supplemental Figure 5. CCL2$^+$ and CCR2$^+$ cells are primarily composed of inflammatory myeloid cells. Frequency of CCL2$^+$CD45$^+$ and CCL2$^+$CD45$^-$ cells among mononuclear cells isolated from the CNS of BLZ945- and vehicle-treated mice with EAE. **B)** Frequency of TNF$^+$, and **C)** MHC II$^+$ cells among CCL2$^+$CD11b$^+$ cells. **D)** Frequency of CCL2$^+$CD45$^+$ and CCL2$^+$CD45$^-$ cells among mononuclear cells isolated from the CNS of anti-CSF-1- and control MAb-treated EAE mice. **E)** MFI of CCL2$^+$ cells among CD45$^+$CCL2$^+$ cells. **F)** Frequency of TNF$^+$, and **G)** MHC II$^+$ cells among CCL2$^+$CD11b$^+$ cells. **H)** Frequency of CCR2$^+$ cells among CD45$^+$ cells that were either CD45^{Hi} vs. CD45^{Lo} in BLZ945- or vehicle-treated EAE mice. **I)** Percentage of MHC II$^+$ among "Other CD11b$^+$ cells" from Fig. 7B. **J)** Frequency of CCR2$^+$ cells among CD45$^+$ cells that were either CD45^{Hi} vs. CD45^{Lo} in anti-CSF-1- or control MAb-treated mice. **K)** Frequency of CCR2$^+$CD11b$^+$ cells among CCL2$^+$ cells. Statistical significance was calculated with two-tailed unpaired t test. Error bars are S.E.M.

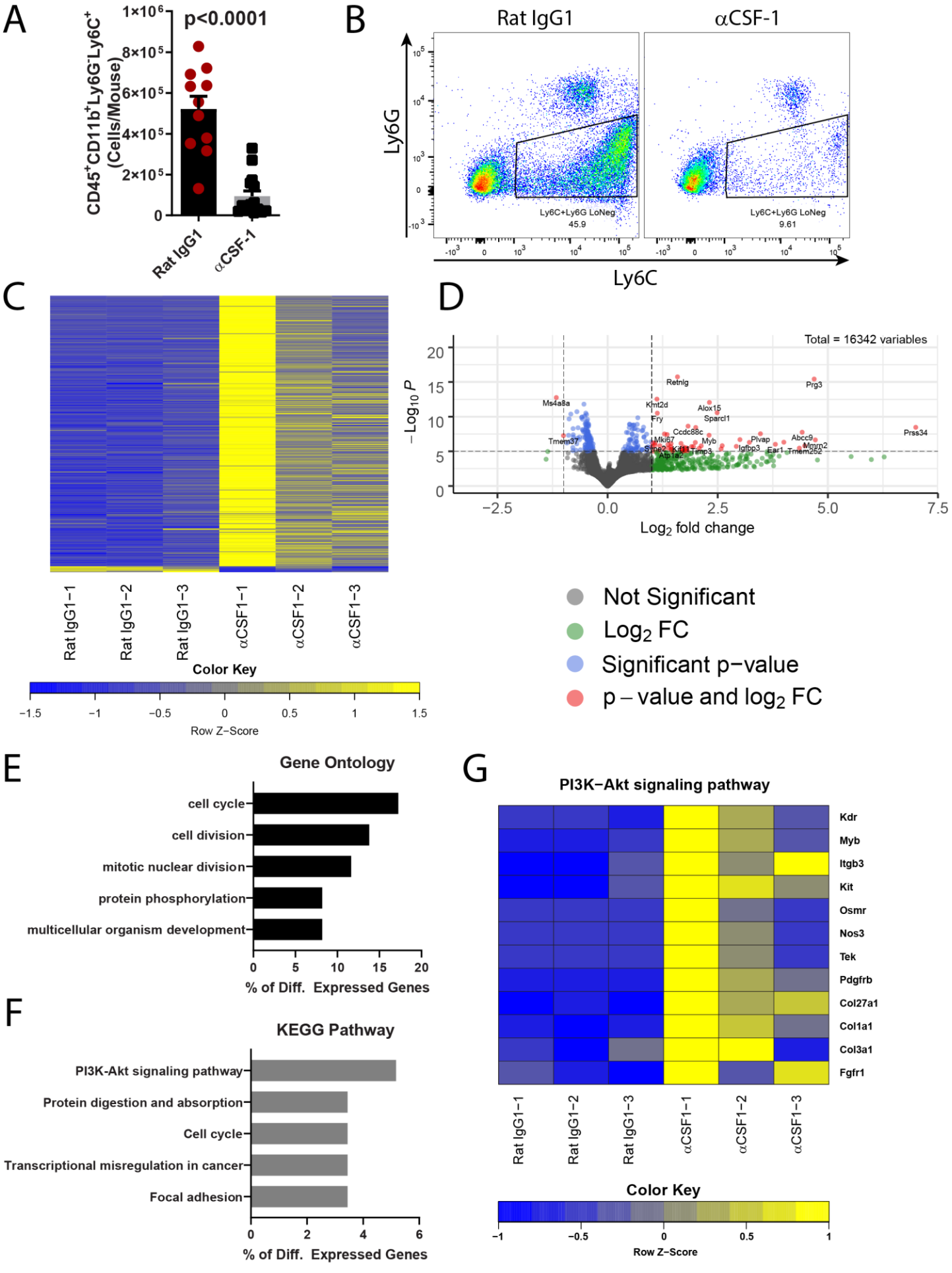

843

Figure 8. Monocytes from the CNS of anti-CSF-1 MAb-treated mice with EAE have a transcriptionally distinct phenotype. EAE was induced in C57BL/6J mice by immunization with MOG_{35-55}. Mice were treated with 200 μg/day of anti-CSF-1 MAb or isotype IgG1 control MAb (n=3/group) from day 11 to 16 p.i. and sacrificed on day 17 p.i. **A)** Numbers of $CD45^{Hi}CD11b^{+}Ly6G^{-}Ly6C^{+}$ monocytes. **B)** Flow cytometry plots showing expression of Ly6C and Ly6G among $CD45^{+}CD11b^{+}$ cells. **C)** Heatmap showing differentially expressed transcripts in monocytes from anti-CSF-1- and isotype MAb-treated mice. Criteria for inclusion in heatmap was expression in all samples, with a p-adjusted value < 0.05 and a $\log_2$ fold change greater/less than ±1. **D)** Volcano plot showing relative expression of transcripts detected in samples from anti-CSF-1- and isotype MAb-treated mice. **E)** Gene ontology and **F)** KEGG pathway terms that were significantly enriched ($p<0.05$) and ranked by percentage of differentially expressed genes (p-adj<0.01). **G)** Heatmap of z-score-normalized TPM data from differentially expressed genes detected from the PI3K-Akt signaling pathway KEGG term.

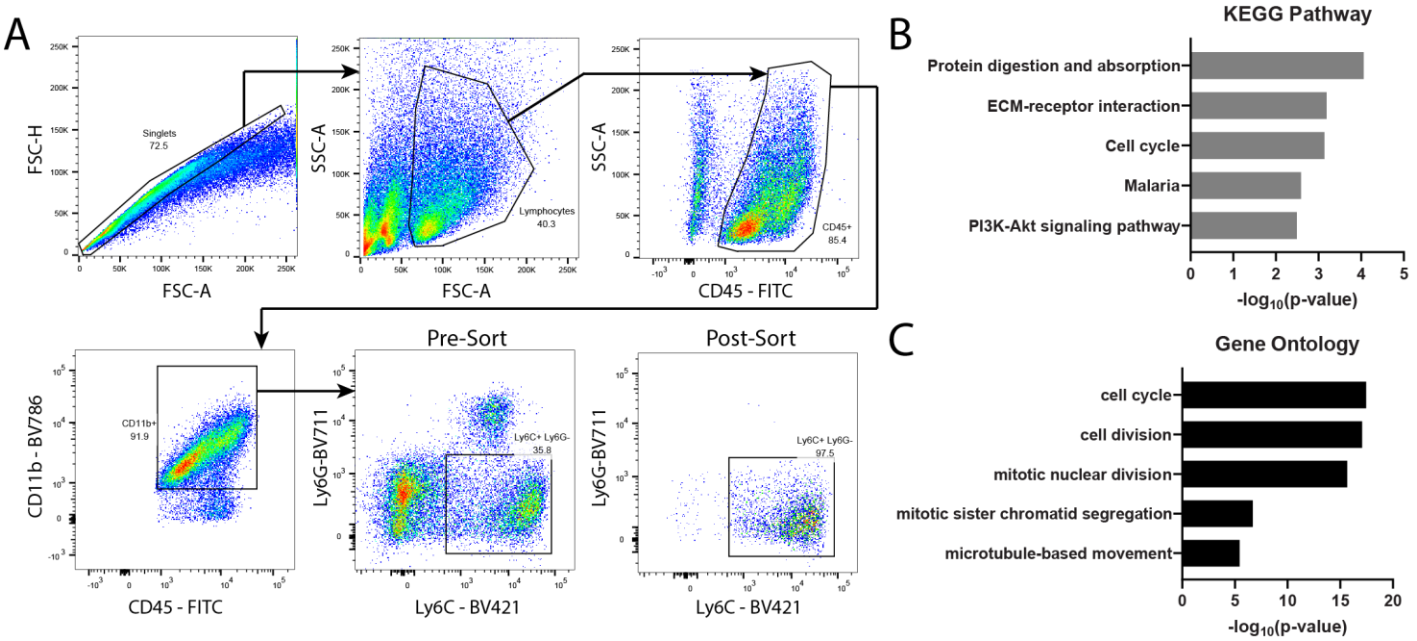

Supplemental Figure 6. Monocytes from the CNS of mice with EAE treated with anti-CSF-1 MAb have distinct transcriptional profile. EAE was induced in C57BL/6J mice by immunization with MOG_{35-55}. Mice were treated with 200 μg/day of anti-CSF-1 MAb or isotype control MAb from day 11 to 16 p.i. and sacrificed on day 17 p.i. **A)** Gating strategy for FACS sorting of $CD45^{Hi}CD11b^{+}Ly6G^{-}Ly6C^{+}$ monocytes/monocyte-derived cells. **B)** Gene ontology and **C)** KEGG pathway terms ranked by significance and generated from differentially expressed genes between monocytes/monocyte derived cells from anti-CSF-1- and isotype control MAb-treated mice.